Selected reprints and preprints

Paper 1 Šedivcová T., Žďánská P.R., Špirko V., Fišer J.: Computed lifetimes of metastable states of CO^{2+}. Journal of Chemical Physics **124** (21): Art. No. 214303 (2006).

Paper 2 Šedivcová T., Špirko V., Fišer J.: Theoretical study of the CS^{2+} dication, Journal of Chemical Physics **125** (16): Art. No. 164308 (2006).

Paper 3 Šedivcová T., Špirko V., Žďánská–Kaprálová P. R.: Radiative properties of the CO^{2+} dication. Journal of molecular spectroscopy: submited.

Paper 4 Šedivcová T., Špirko V.: Potential energy and transition dipole moment functions of C_2^-. Molecular Physics **104** (13-14): 1999–2005 (2006).

omputed lifetimes of metastable states of CO^{2+}

T. Šedivcová, P. R. Žďánská, and V. Špirko[a]
Department of Molecular Modeling, Center for Biomolecules and Complex Molecular Systems, Institute of Organic Chemistry and Biochemistry, Academy of Sciences of the Czech Republic, Flemingovo náměstí 2, 166 10 Prague 6, Czech Republic

J. Fišer
Faculty of Science, Department of Physical and Macromolecular Chemistry, Charles University, Hlavova 2030, 128 40 Prague 2, Czech Republic

(Received 16 February 2006; accepted 29 March 2006; published online 2 June 2006)

Highly correlated internally contracted multireference configuration interaction wave functions are used to calculate the potential energy and spin-orbit coupling functions for the lowest electronic states of CO^{2+} dication. Using these functions, the positions and lifetimes of the corresponding vibronic states are evaluated by means of log-phase-amplitude, stabilization, and complex-scaling methods within the framework of a multichannel Schrödinger analysis. For the first time in the literature, the calculated lifetimes are in good agreement with the experiment, thereby proving the reliability of the predicted characteristics and adequacy of the used theory for a theoretical study of other molecular dications. © *2006 American Institute of Physics*. [DOI: 10.1063/1.2198835]

INTRODUCTION

Small, multiply charged molecular ions are of topical nterest in science, especially due to their roles in extreme nvironments, such as planetary atmospheres, circumstellar nvelopes, and interstellar regions (for more details see, e.g., Refs. 1–5). Generally, due to the strong electrostatic repulsion of their charged centers, the multiply charged ions are hermochemically unstable. However, quite frequently, hemical bonding can overcome this repulsion and make hese ions fairly stable or, at least, metastable. A key stability aspect concerns the relative positions of the potential energy asymptotes of the ions and the corresponding charge-separated fragments and the positions of the molecular vibronic levels. The stability of individual molecular states also depends strongly on the shape of the potential energy curves, their relative positions, and interstate electronic couplings. Consequently, the actual lifetimes acquire values which may vary over a fairly wide range of values. For instance, experimentally determined lifetimes of CO^{2+} range from a few tenths of a nanosecond to several seconds.[6–10]

From the dynamic point of view, the lifetimes are determined by the tunnelings through the potential barriers and by the predissociations mediated by the electronic couplings, such as the spin-orbit couplings (see, e.g., Ref. 8). The theoretical evaluation of the lifetimes is thus limited only by the knowledge of the potential energy and electronic coupling functions. In principle, these potentials can be derived from vibrationally resolved spectral data. Presently, such data are accessible mainly by means of the threshold photoelectrons coincidence (TPEsCO) technique,[11,12] the time-of-flight photoelectron-photoelectron coincidence (TOF-PEPECO) method,[13] the time-of-flight Doppler-free kinetic energy release (DFKER) spectroscopy,[7] the double charged transfer (DCT) technique,[14] and, ideally, rotationally resolving optical spectroscopy.[15–17] So far, however, mostly due to the scarcity and limited accuracy of the available experimental data, no experimental "multichannel" potentials have been derived from the experiment. A natural way of overcoming this situation is the theoretical modeling based on a highly accurate *ab initio* evaluation of the molecular potentials and their critical testing by comparison with the experiment. Although it is extremely difficult to calculate these potentials with spectroscopic accuracy, the *ab initio* approach has been adopted in a long series of theoretical studies and has been found to be useful in many respects. In the case of CO^{2+}, for instance, the comprehensive sets of potential energy functions (PEF's) were published by Wetmore *et al.*,[18] Larsson *et al.*,[19] and Eland *et al.*[20] The most accurate potentials are those of Eland *et al.* who rely on a full valence multireference configuration interaction (MRCI) treatment. These potentials provide very good agreement between the experiment and the theory regarding spectroscopic constants, photo-double-ionization spectra, and band origins of the vibrational progressions of several quasibound electronic states. Veseth[21] computed vibrationally resolved partial cross sections for photoionization of CO^+ and from these results deduced information on the equilibrium internuclear distance of the CO^{2+} $^3\Pi$ ground state. The spin-orbit couplings (SOC's) among the three lowest electronic states $X\,^3\Pi$, $a\,^1\Sigma^+$, and $^3\Sigma^-$ of CO^{2+} were calculated by Andersen *et al.*[8] as residues of linear response functions of multiconfigurational self-consistent-field (SCF) states.[22]

Using their *ab initio* data, Andersen *et al.*[8] have completed their study by evaluating the electronic predissociation rates of the vibrational levels of the $X\,^3\Pi$ and $a\,^1\Sigma^+$ electronic states from the solution of the exterior complex dilated multichannel Schrödinger equation, describing nuclear motion. The same *ab initio* data were also used by Bouhnik *et al.*[9] in an approximate evaluation of the sought rates by

[a]Electronic mail: spirko@marge.uochb.cas.cz

 © 2006 American Institute of Physics

Downloaded 04 Jun 2006 to 130.183.82.42. Redistribution subject to AIP license or copyright, see http://jcp.aip.org/jcp/copyright.jsp

neans of the Fermi-Wentzel golden rule formula (the vibra-ional wave functions used in these calculations were ob-ained using the log-amplitude-phase method[23]). Interest-ngly, the approximate values of the rates were found in close greement with their "exact" counterparts. Both sets of the neoretical data, however, are in striking disharmony with the xperiment. Therefore, aiming to resolve this confusion, we nd it desirable to calculate the predissociation rates once gain, using a more accurate theoretical procedure and in-olving a more extended set of electronic states. The re-uired potential energy and spin-orbit coupling functions are valuated using internally contracted multireference configu-ation interaction (icMRCI) wave functions. The approxi-nate "one-dimensional" tunneling rates/lifetimes are evalu-ted using the log-phase-amplitude method,[23] and the umerically exact (multichannel) predissociation rates/ fetimes accounting for the spin-orbit interactions are calcu-ted using the stabilization[24–26] and complex-scaling ethods.[27,28] The latter computational approaches have roved to be fairly reliable in our previous treatment of the asibound states of van der Waals molecules[29–31] and pre-issociation resonances of diatomic molecules.[32] All the entioned methods are described briefly in Sec. II.

. COMPUTATIONAL METHODS

. Potential energy curves and spin-orbit couplings

Ab initio calculations were carried out using the MOLPRO ite of *ab initio* programs.[33] The atomic orbital basis sets ere cc-pV*X*Z, $X=5,6$.[34] The molecular orbitals for the CI eatment of CO^{2+} were obtained in both the one-state and e state-averaged complete-active-space SCF (CASSCF) lculations with equal weights for the participating states of e same spin multiplicity in C_{2v} symmetry. With the cc-V6Z basis set, the full active space consisted of $1\sigma-6\sigma$, π, and 2π orbitals with all electrons (AE) correlated. This d to a total of 5220 configuration state functions (CSF's) in e $X\,^3\Pi$, 5154 in the $A\,^3\Sigma^+$, and, e.g., 5196 in the $^3\Sigma^-$ state. e PEF's were calculated using the icMRCI method.[35,36] e number of uncontracted configurations was about 4.1 $10^8-7.9\times10^8$. In calculating excitation energies and KER, generalized Davidson correction[37] was employed.

For the sake of comparison, some PEF's of CO^{2+} were lculated, using the spin-restricted coupled cluster method th singles, doubles and a perturbative estimate of triple citations [RCCSD(T)].[38,39] The SO integrals were evalu-d with the icMRCI wave functions, using the Breit-Pauli erator, as implemented in the MOLPRO code. Due to the nitation of this program, only the *spdf* orbital subset of the -pV5Z basis set with the valence electrons correlated was ployed in the SO calculations.

Resonance calculations

The energies of vibronic states were obtained by numeri-l integration of the Schrödinger equation of the system miltonian $\hat{H}$. The positions and lifetimes of the quasi-und levels of CO^{2+} were evaluated using three different proaches: the log-amplitude-phase method for solving one-dimensional problems (SO interaction disregarded) and the stabilization and complex-scaling methods based on the coupled treatment of the electronic states by means of SO interaction.

The log-amplitude-phase method of Sidky and Ben-Itzhak[23] is a modification of the earlier Milne method.[40] This approach which takes advantage of the oscillatory structure of the wave function provides an efficient way for locating resonances: the local maxima in the energy derivative of a phase are identified as resonance peaks, the resonance widths are calculated from the Breit-Wigner line shape formula.

The stabilization method[24–26] is based on the fact that the wave functions for resonance states closely resemble the wave functions for bound states. The energies of resonance states are stable when a basis set parameter, e.g., the dissociative coordinate R, is varying. In contrast, the energies associated with the nonresonant states increase monotonically as R decreases. So the key idea of the boxing variant of the method is a repeated diagonalization of an appropriate Hamiltonian $\hat{H}$ in a series of enclosing boxes with their varying box size R: $R_0 \leq R \leq R_0+\Delta R$. Plots of the eigenfunction of the Hamiltonian $E(R)$ as a function of R are known as the stabilization diagram.

The primary result of this method is an average density of states $\rho(E)$, from which the resonance energies and widths can be determined by the Lorentzian fitting. The average density of states was evaluated as

$$\rho(E) = -1/\Delta R \sum_n (dE_n(R)/dR)^{-1}|_{E_n=E}. \tag{1}$$

The total phase shift $\phi(E)$ has been obtained from the stabilization diagram using the formula

$$\phi(E) = \sum_n \phi_n(E), \tag{2}$$

where ϕ_n is the contribution from the nth eigenvalue $E_n(R)$ defined by

$$\phi_n(E) = \begin{cases} 0 & \text{for } E < E_n(R+\Delta R) \\ \pi\dfrac{R+\Delta R - R_n(E)}{\Delta R} & \text{for } E_n(R+\Delta R) < E < E_n(R) \\ 1 & \text{for } E > E_n(R), \end{cases} \tag{3}$$

where R is the current size of the coordinate box and $R_n(E)$ is a function obtained using the numerical inversion of $E_n(R)$. Using the Breit-Wigner formula, the resonance energies and widths have been obtained by fitting $\phi(E)$ near a resonance energy to

$$\phi(E) = \arctan\left(2\frac{E-E_{\text{res}}}{\Gamma_{\text{res}}}\right) + \phi_b(E), \tag{4}$$

where E_{res} and Γ_{res} are the energy and the width of the resonance and $\phi_b(E)$ is the background term. The width of a metastable state is related to its lifetime through the uncertainty relationship $\tau=\hbar/\Gamma$.

ownloaded 04 Jun 2006 to 130.183.82.42. Redistribution subject to AIP license or copyright, see http://jcp.aip.org/jcp/copyright.jsp

In the complex-scaling method,[27] the sought resonance characteristics are obtained from complex eigenvalues of a complex-scaled Hamiltonian. The advantage of this method is that the resonance solutions are square integrable, so the Schrödinger equation can be solved by bound-state techniques. The complex-scaled Hamiltonian $\hat{H}_\theta(x)$ is obtained from the physical Hamiltonian $\hat{H}(x)$ by complex scaling of the coordinate x, such that $\hat{H}_\theta(x)=\hat{H}(xe^{i\theta})$, where θ is a complex-scaling parameter $0\leq\theta<\pi/4$. The complex-scaled Hamiltonian for the CO^{2+} dissociation is obtained by the complex transformations of the kinetic energy operator, potential, and SO coupling, such that

$$\hat{H}_\theta(x) = -e^{-2i\theta}\frac{\hbar^2}{2\mu}\frac{d^2}{dx^2} + V(xe^{i\theta}), \tag{5}$$

with approach that the potentials are coupled between each other by the SO operator. The complex transformations of SO coupling is straightforward also as $\hat{C}_\theta(x)=C(xe^{i\theta})$. Resonances are obtained as solutions of $\hat{H}_\theta(x)$ and are characterized by θ-independent complex eigenvalues. The complex resonance eigenvalues,

$$\epsilon = E_{\rm res} - \frac{i}{2}\Gamma_{\rm res}, \tag{6}$$

define the resonance positions $E_{\rm res}$ and widths $\Gamma_{\rm res}$, respectively. Resonance states appear in the spectrum of $\hat{H}_\theta(x)$ for θ being larger than a critical value given by

$$\theta_c = \frac{1}{2}\arctan\frac{\Gamma_{\rm res}}{2E_{\rm res}}. \tag{7}$$

The eigenfunctions and eigenvalues of $\hat{H}_\theta(x)$ are obtained in a finite box using a Fourier basis set. Resonance eigenvalues are obtained in the finite basis set as the stationary points with respect to variation of the scaling parameter,[27]

$$\left.\frac{\partial E_{\rm res}}{\partial\theta}\right|_{\theta_{\rm stat}} = \left.\frac{\partial\Gamma_{\rm res}}{\partial\theta}\right|_{\theta_{\rm stat}} = 0. \tag{8}$$

In order to enable the construction of the complex-scaled Hamiltonian [Eq. (5)], the potential energy $V(x)$ and SO coupling $C(x)$ are represented by analytical functions which allow for their analytical continuation to the complex plane $x\to xe^{i\theta}$. The potential and SO coupling Hamiltonian matrices are calculated using a discrete variable representation.[28]

II. RESULTS AND DISCUSSION

The PEF's of the ground and eight excited electronic states of CO^{2+}, calculated at the icMRCI/cc-pV6Z/AE level, are displayed in Fig. 1. Qualitatively, it is a very similar picture to that given in Ref. 20. Moreover, it includes the repulsive $^3\Delta$ and the quasibound $e\ ^1\Sigma^+$ states. For most states considered, we have been able to calculate the PEF's in the range $1.7\leq R\leq 10.2$ bohrs. The spectroscopic constants derived from these PEF's are very similar to those of Eland *et al.*[20] obtained by the same method with all valence electrons correlated. For all states, our equilibrium internuclear

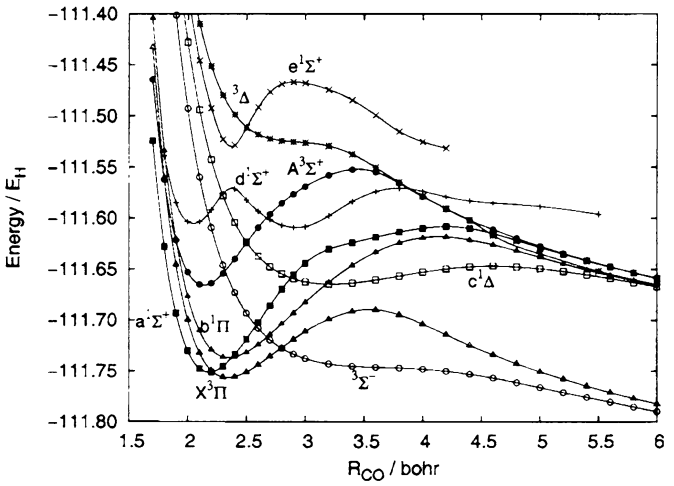

FIG. 1. The icMRCI potential energy functions of the nine lowest electronic states of CO^{2+} dication.

distances are slightly lower (by about 0.002–0.009 Å) than those in Ref. 20. It should be noted that Veseth[21] deduced (using the many-body calculations) the equilibrium internuclear distance of 1.238 Å for the ground state $X\ ^3\Pi$ of CO^{2+} from photoionization cross sections of CO^+; this value is very close to the icMRCI/V6Z/AE and RCCSD(T)/V6Z/AE results, 1.2392 and 1.2377 Å, respectively. Our harmonic frequencies are by about 10–35 cm^{-1} higher than the previous theoretical values[20] with an exception of the $d\ ^1\Sigma^+$ state having the double-minimum potential with lower frequency for the outer potential well, $\omega_e=1099.3\ cm^{-1}$, comparing with 1125.6 cm^{-1} of Eland *et al.*[20] All the calculated spectroscopic constants are presented in Table A in the supplementary material.[41]

The quality of the computational treatment can also be assessed by a comparison of the computed band origins for the vibrational progressions of several electronic states of CO^{2+} (excitation energies from the CO ground state) with the previously reported experimental and theoretical data (see Table I). The agreement of our icMRCI+Q values with the TOF-PEPECO data seems to be even slightly better than that obtained by Eland *et al.*[20] for their unshifted theoretical values. Another important quantity which can be compared with the experiment and used to characterize the decay mechanism is the kinetic energy released upon unimolecular dissociation of CO^{2+}. In this connection, it is noteworthy that only the ground state $^3\Pi$ and the purely repulsive $^3\Sigma^-$ state have the lowest common asymptotic atomic limit $C^+(^2P_u)+O^+(^4S_u)$. Using the one-state calculation of the $X\ ^3\Pi$ state at the icMRCI+Q/V6Z/AE level of theory, we have been able to obtain energies of up to $R=250$ bohrs. An extrapolation to infinity was performed using an assumed $1/R$ functional form. For the ($X\ ^3\Pi$, $v=2$), ($a\ ^1\Sigma^+$, $v=1$), ($b\ ^1\Pi$, $v=1$), and ($A\ ^3\Sigma^+$, $v=0$) states, we obtained $E_k=5.654$, 5.711, 5.829, and 7.802 eV, which are in very good agreement with the experimental data of Lundqvist *et al.*,[7] 5.655, 5.713, 5.841, and 7.833 eV, respectively. It should be mentioned that the experimental KER value $E_k=5.713$ eV, originally associated with the $a\ ^1\Sigma^+$, $v=0$ state,[7] was later reassigned by Hochlaf *et al.*[11] to the $v=1$ state.

Downloaded 04 Jun 2006 to 130.183.82.42. Redistribution subject to AIP license or copyright, see http://jcp.aip.org/jcp/copyright.jsp

BLE I. Band origins for vibrational progressions of the CO^{2+} dication determined from experiment and *ab initio* calculations. The energy zero in the ulations is the $X\,^1\Sigma^+$, $v=0$, $J=0$ state of CO. The data are in eV.

	$X\,^3\Pi$	$a\,^1\Sigma^+$	$b\,^1\Pi$	$A\,^3\Sigma^+$	$d\,^1\Sigma^+$	$c\,^1\Delta$	$e\,^1\Sigma^+$
EsCO[a]	41.294±0.01	41.500[b]	41.814	43.826[c]	45.480		
KER[d]	41.300[e]	41.490[f]	41.818	43.810	45.470		
EsCO[g]	41.324±0.01[h]	41.525±0.01	41.847±0.01				
F-PEPECO[i]	41.275±0.03	41.438±0.02	(41.780)	43.799±0.03	45.461±0.03		
T[j]		41.52±0.05			45.51±0.05		
nd *et al.*[k]	41.064	41.252	41.585	43.622	45.434	43.581	
fRCI+Q/AE[l]	42.229	41.370[m]	41.749	43.722	45.343	43.590	46.899

eference 12.
e reassignment suggested in Ref. 11 was used. (The vibration sequence begins one quantum lower than originally assigned in Ref. 12). The position of the 0 level has been calculated using ω_e and $\omega_e x_e$ of Ref. 11.
e reassignment suggested in Ref. 7 was used. The original value presented in Ref. 12 was 43.573 eV.
eference 7.
e $v=2$ level was observed. $E(v=0)$ has been calculated by subtracting the TPEsCO separation (Ref. 12) from $E(v=2)$.
e value reassigned by Hochlaf *et al.* (Ref. 11). The position of the $v=0$ level has been calculated using ω_e and $\omega_e x_e$ of Ref. 11.
eference 11.
$v=0$) calculated from E_0 using the formula $E(0)=E_0+\omega_e/2-\omega_e x_e/4$ with the data given in Table 2 of Ref. 11. See also Ref. 6.
eference 13.
eference 14.
eference 20. Unshifted values.
l electrons correlated in the CASSCF/icMRCI+Q calculations. The energies of the $X\,^3\Pi$, $b\,^1\Pi$, and $A\,^3\Sigma^+$ states obtained using the one-state calculations. he one-state icMRCI+Q calculation yields the value 41.394 eV.

The SO couplings among the six lowest dicationic states $^3\Pi$, $a\,^1\Sigma^+$, $b\,^1\Pi$, $^3\Sigma^-$, $A\,^3\Sigma^+$, and $c\,^1\Delta$ as a function of ternuclear distance are displayed in Fig. 2 (some spin-orbit atrix elements are zero due to symmetry). The most strik- g feature of these interactions is the R dependence of the atrix element connecting the $^3\Sigma^-$ and $^1\Sigma^+$ states, which is far the largest in the range $3.2<R<4.6$ bohrs. In the nited interval of the internuclear C–O separations, similar havior has also been found by Andersen *et al.*[8] By con- ast, the SO $a\,^1\Sigma^+-X\,^3\Pi$ and $^3\Sigma^--X\,^3\Pi$ interactions calcu- ted using the icMRCI method differ from those of Ander- n *et al.*, although the (global) minimum of the former SO urve lies at a similar internuclear distance (~3 bohrs).

The tunneling (one dimensional) widths of the vibra- onal levels supported by the quasibound adiabatic poten- als were calculated using the log-phase-amplitude method f Sidky and Ben-Itzhak.[23] For the $X\,^3\Pi$, $a\,^1\Sigma^+$, $b\,^1\Pi$, and $A\,^3\Sigma^+$ states, these data are very close to the previously reported values of Eland *et al.*[20] Our calculations show that both the extension of the basis set (V5Z→V6Z) and the inclusion of all electrons into correlation mostly decreases the width of the vibrational states. These results confirm the well-known fact that tunneling lifetimes are extremely sensitive to the basis set and the details of the potential. The tunneling lifetimes for some lower vibrational levels of the $c\,^1\Delta$, $d\,^1\Sigma^+$, and $e\,^1\Sigma^+$ states (cf. Table II) are long enough for tunneling through the potential barrier to be partly responsible for the dissociation of CO^{2+} from these states. However, as noted by Larsson *et al.*,[15] it is difficult to populate the low-lying vibrational levels due to the long-range bonding nature of the $c\,^1\Delta$ state. For the $d\,^1\Sigma^+$ state, the tunneling lifetimes are supposed to be of the same order of magnitude as the electronic predissociation rates.[7,9] However, it should be kept in mind that for quasibound electronic states, where the spin-orbit induced predissociation is possible, the tunneling widths represent lower bounds to real widths. For the $e\,^1\Sigma^+$ state, the tunneling mechanism could play a role in a predissociation dynamics, since the SOC

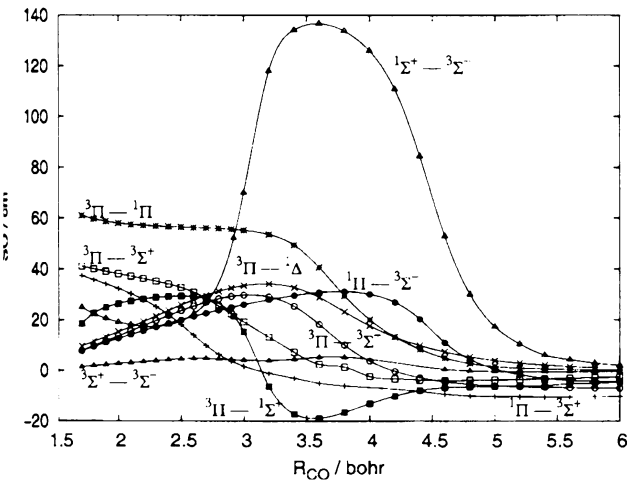

IG. 2. Spin-orbit couplings between the six lowest electronic states of CO^{2+} dication.

TABLE II. Tunneling widths (in cm^{-1}) for the vibrational levels of the $c\,^1\Delta$, $d\,^1\Sigma^+$, and $e\,^1\Sigma^+$ electronic states of CO^{2+}. Only widths greater than 10^{-25} are shown.

v	$c\,^1\Delta$	$d\,^1\Sigma^{+a}$	$e\,^1\Sigma^+$
1			3.380×10^{-24}
2	5.779×10^{-20}		2.303×10^{-16}
3	1.755×10^{-15}		1.309×10^{-9}
4	2.161×10^{-11}	1.350×10^{-16}	8.349×10^{-4}
5	1.258×10^{-7}	1.020×10^{-9}	16.00
6	3.062×10^{-4}	1.481×10^{-5}	
7	2.585×10^{-1}	2.644×10^{-2}	
8	26.49	9.276	

[a]Tunneling through the outer barrier is calculated.

Downloaded 04 Jun 2006 to 130.183.82.42. Redistribution subject to AIP license or copyright, see http://jcp.aip.org/jcp/copyright.jsp

TABLE III. Energy positions in cm^{-1} of the lowest vibronic resonances of CO^{2+}.

State	v	Reference 11[a,b]	Reference 12[b,c]	Stabilization method	Complex scaling
$X\,^3\Pi$	0	677.1	806.7	732.7	732.5
	1	2004.7	2258.3	2138.8	2101.3
	2	3296.8	3484.3	3550.2	3549.5
	3	4553.4	⋯	4885.1	4884.5
	4	5774.5	⋯	6168.9	6168.9
	5	6960.2	⋯	7401.5	7401.6
$a\,^1\Sigma^+$	0	2298.7	⋯[d]	2175.0	2169.6
	1	3911.9	4081.1	4062.5	4044.9
	2	5524.9	6000.7	5941.6	5942.4
	3	7138.0	7670.3	7784.6	7759.0
$b\,^1\Pi$	0	4891.8	5000.6	5030.6	5030.8
	1	6287.1	6533.1	6512.6	6511.4
	2	7617.9	8009.1	7960.8	7959.0

[a]Obtained from the values in Table 2 of Ref. 11 using the formula $E(v)=E_0+\omega_e(v+1/2)-\omega_e x_e(v+1/2)^2$.
[b]The energy zero is E_0 ($X\,^3\Pi$).
[c]Calculated from the values in Table 3 and E_0 (Table 4) of Ref. 12.
[d]Experimental data reassigned by Hochlaf *et al.* (Ref. 11).

egrals between the $e\,^1\Sigma^+$ and $^3\Delta$ states are zero due to nmetry. As can be seen from Table II, the tunneling lifeies for the $v=2$ and 3 vibrational states are of the order of lliseconds and nanoseconds, respectively.

The real (multichannel) linewidths were obtained by ving the system of the coupled channel Schrödinger equaons,

$$\frac{d^2\mathbf{y}(R)}{dR^2}=[\mathbf{V}(R)-E\mathbf{I}]\mathbf{y}(R), \tag{9}$$

ere the diagonal and off-diagonal elements of the potential ergy matrix $\mathbf{V}(R)$ consist of the adiabatic potential energy ctions (Fig. 1) and the SO interactions (Fig. 2), respecely, $y(R)$ is a column vector, and $\mathbf{I}$ is the unity matrix. To get fully converged results for the observed states, the six lowest electronic states $X\,^3\Pi$, $a\,^1\Sigma^+$, $^3\Sigma^-$, $b\,^1\Pi$, $c\,^1\Delta$, and $A\,^3\Sigma^+$ had to be involved.

In the actual stabilization calculations, R_0 was fixed at 1.7 bohr, R was varied from 1.7 to 6.1 bohrs by the increment of 0.001 bohr, and Eq. (9) was solved using the renormalized Numerov method.[42] The calculated positions and lifetimes of the probed states are collected in Tables III and IV. A typical detail of the global stabilization diagram and the corresponding density of states are illustrated in the supplementary material[41] by Figs. A and B, respectively.

The complex-scaling calculations were performed using polynomially smoothed potential and SO coupling functions (see Eqs. A and B and Tables B and C in the supplementary

BLE IV. Lifetimes τ (μs) of the lowest vibronic resonances of CO^{2+}.

DFKER (Ref. 7)	SR (Ref. 8)	DP[a] (Ref. 6)	TDFI (Ref. 9)	Theory (Ref. 8)	Theory (Ref. 9)	Stabilization method	Complex scaling
			$^3\Pi$ state				
$\gg 3$	$>3.8\times10^6$	$\gg 10$		2×10^4	0.77×10^4	>10	>10
>3	8×10^{2b}	>10		0.3	0.17	>10	>10
<0.1		0.2 ± 0.1	(0.32 ± 0.22)		0.29×10^{-3}	0.61	3.9
<0.1		<0.1				1.2×10^{-3}	5×10^{-3}
<0.1						3.2×10^{-4}	1.2×10^{-4}
						8.9×10^{-6}	15×10^{-6}
			$a\,^1\Sigma^+$ state				
	6×10^{3b}	>10		2.0	0.78	>10	>10
0.6 ± 0.1		$0.7^{+0.2}_{-0.1}$	0.67 ± 0.05	1.3×10^{-3}	8.8×10^{-3}	0.67	5
<0.1						2.8×10^{-2}	15×10^{-2}
						8.7×10^{-4}	2×10^{-4}
			$b\,^1\Pi$ state				
<0.1		$0.2^{+0.15}_{-0.2}$	0.026 ± 0.005			8.3	23
<0.1		<0.1				2.2×10^{-4}	15×10^{-4}
<0.1						1.01×10^{-5}	0.5×10^{-5}

ie data were taken with $^{13}C^{16}O^{2+}$.
ntatively assigned by Hochlaf *et al.* (Ref. 11).

Downloaded 04 Jun 2006 to 130.183.82.42. Redistribution subject to AIP license or copyright, see http://jcp.aip.org/jcp/copyright.jsp

:rial[41]). The polynomial approximation is not fully quan- ve, especially for the SO couplings, and limits thus ac- cy of the calculated characteristics. As a matter of fact, :orresponding errors affect the sought characteristics for ɔbserved states more than the couplings of these states the $c\ ^1\Delta$ and $A\ ^3\Sigma^+$ states. Consequently, the latter states : excluded from our scheme. The actual calculations : performed variationally using 300 basis functions, 1.7 ≤7.2 bohrs, and θ varying from 0.0001 to 0.06. The ılated energy positions and lifetimes are collected to- er with their stabilization counterparts in Tables III and The corresponding energy spectrum of the complex- :d Hamiltonian and an example of a typical θ trajectory ;hown in the supplementary material[41] (Figs. C and D). The calculated vibrational energies of the probed ($X\ ^3\Pi$, $^+$, and $b\ ^1\Pi$) electronic states are compared in Table III the experimental values of Hochlaf *et al.*[11] and Dawber *l.*[12] It can be seen that for the majority of states the ıational energies obtained by both theoretical methods :r very slightly and lie between the respective experimen- ıata.

The main result of this study, i.e., the lifetimes of the ıational states of the lowest electronic states, is reported compared with the experimental and other theoretical in Table IV. It should be noted that both the stabilization complex-scaling methods can provide accurate estimates for lifetimes shorter than 10 μs. Yet, it is still possible educe from the calculations that the $X\ ^3\Pi$, $v=0$ and v levels are the only quasistable levels with lifetimes of h longer than 10 μs. This qualitative result is in a good ement with the limit $\tau>3.8$ s, determined by means of a 'y ion storage ring[8] and with $\tau=0.8$ ms measured by ersen *et al.*[8] and reassigned by Hochlaf *et al.*,[11] respec- y. The lifetime $\tau(X\ ^3\Pi, v=2)=0.61$ μs obtained using more accurate stabilization method compares favorably $\tau=0.2\pm0.1$ μs which relied upon double photoioniza- using synchrotron radiation[6] and 0.32 ± 0.22 μs deter- :d using the 3D-fragment imaging technique.[9] For this ıational state, the complex scaling yields a somewhat er value (3.9 μs). The lifetime of higher vibrational lev- decreases dramatically as their energy increases. The puted values for $v=3$ and 4 states are consistent with the :rimental upper bounds determined by the DFKER troscopy[7] and the double photoionization.[6] On the con- , the theoretical estimates obtained by Larsson *et al.*,[15] ersen *et al.*,[8] and Bouhnik *et al.*[9] are in a profound dis- ıony with experiment.

For the $a\ ^1\Sigma^+$, $v=0$ state, our computed lifetimes are ı much longer than 10 μs, being in accord with τ ns measured by Andersen *et al.*[8] and reassigned by ılaf *et al.*[11] Among all studied vibronic states of CO^{2+}, nost information is reported for the $v=1$ ($a\ ^1\Sigma^+$) vibra- ıl state. The experimental values range from o 0.7 μs. The stabilization method gives a lifetime of μs, which is, fortuitously, the same as that based on the ıltaneous measurement of kinetic energy release and life- by Bouhnik *et al.*[9] The complex-scaling procedure ı leads to a higher value (5 μs) than the stabilization ıod.

In the case of the $b\ ^1\Pi$, $v=0$ state the precise value of 0.026 ± 0.005 μs is provided by Bouhnik *et al.*[9] The double photoionization method yields a much higher value, 0.20 ± 0.15 μs. However, the corresponding error bars are rather high. As a matter of fact, our theoretical estimates are even larger (8.3 and 23 μs), being thus the only data of this study which are in a factual disharmony with experiment. Similarly to the $X\ ^3\Pi$ and $a\ ^1\Sigma^+$ states, the lifetimes for higher vibrational levels rapidly decrease as their energy increases.

The most striking feature governing the decay and dynamics of the low-lying vibrational states is the crossing of the PEC's of the respective quasibound states by that of the purely repulsive $^3\Sigma^-$ state. For the three lowest electronic states $X\ ^3\Pi$, $b\ ^1\Pi$, and $a\ ^1\Sigma^+$, the crossing points lie at $R\sim2.8$, 2.6, and 2.7 bohrs, respectively. In this region, at about $R\sim2.7$ bohrs, the values of the spin-orbit coupling integrals $\langle X\ ^3\Pi, m_s=1|L_yS_y|\ ^3\Sigma^-, m_s=0\rangle$, $i\langle a\ ^1\Sigma^+, m_s=0|L_zS_z|\ ^3\Sigma^-, m_s=0\rangle$, and $\langle b\ ^1\Pi, m_s=0|L_yS_y|\ ^3\Sigma^-, m_s=1\rangle$ are similar; they range between 22 and 28 cm^{-1}. However, the second integral begins to rise sharply with increasing R and at about 3.6 bohrs it reaches its highest value of 136 cm^{-1}. Whereas the $X\ ^3\Pi$, $b\ ^1\Pi$, and also $A\ ^3\Sigma^+$ and $d\ ^1\Sigma^+$ states predissociate directly by the spin-orbit coupling with the $^3\Sigma^-$ state, the excited $a\ ^1\Sigma^+$ state decays mainly by indirect predissociation[43] because of mixing between the $X\ ^3\Pi$ and $a\ ^1\Sigma^+$ states.[8,9] This is supported by the fact that the $a\ ^1\Sigma^+$, $v=0$ and $X\ ^3\Pi$, $v=1$ states, located near the crossing point, are almost degenerate and also by the relatively large value of the SO matrix element $\langle X\ ^3\Pi, m_s=1|L_yS_y|a\ ^1\Sigma^+, m_s=0\rangle$ (~33 cm^{-1}) in the crossing region. It is high enough to allow such predissociation.

Summarizing, we have obtained the first complete consistent sets of the theoretical lifetimes for 13 low-lying vibronic states of the CO^{2+} dication. The spin-orbit induced lifetimes calculated by the stabilization method are in reasonable agreement with the experimental data in contrast to the theoretical lifetimes reported earlier.

IV. CONCLUSIONS

The CASSCF/icMRCI wave functions were used to calculate the potential energy curves and spin-orbit couplings of the CO^{2+} dication. These results were employed in calculating the positions and lifetimes of the vibrational levels of the $X\ ^3\Pi$, $a\ ^1\Sigma^+$, and $b\ ^1\Pi$ electronic states using the stabilization, complex-scaling, and log-amplitude-phase methods. The first two approaches taking into account spin-orbit interaction yielded lifetimes in qualitative accord with the experimental data, the stabilization method even in a semi-quantitative agreement. While the lowest vibrational levels ($v=0-7$) of the $X\ ^3\Pi$, $a\ ^1\Sigma^+$, $b\ ^1\Pi$, and $A\ ^3\Sigma^+$ states are practically stable against tunneling dissociation, the tunneling lifetimes for some of the lower vibrational levels ($3\leq v\leq7$) of the $c\ ^1\Delta$, $d\ ^1\Sigma^+$, and $e\ ^1\Sigma^+$ states have the tunneling lifetimes ranging between seconds and nanoseconds. However, the calculated lifetimes confirm that the spin-orbit induced predissociation is a dominant decay mechanism for CO^{2+}.

wnloaded 04 Jun 2006 to 130.183.82.42. Redistribution subject to AIP license or copyright, see http://jcp.aip.org/jcp/copyright.jsp

ICKNOWLEDGMENTS

The authors wish to thank the computer MetaCenter for ime allocation. The study was supported by the Grant igency of the Academy of Sciences of the Czech Republic Grant Nos. A400550511, 1ET400400410, and JB100550501), the Grant Agency of the Czech Republic Grant Nos. 203/06/0420, and 203/05/H001), and the Minis- y of Education (Grant No. LC512); it was also a part of the esearch project Z4 055 0506.

[1] D. Schröder and H. Schwarz, J. Phys. Chem. A **103**, 7385 (1999).
[2] Z. Herman, Int. Rev. Phys. Chem. **15**, 299 (1996).
[3] S. D. Price, J. Chem. Soc., Faraday Trans. **93**, 2451 (1997).
[4] S. G. Cox, A. D. J. Critchley, P. S. Kreynin, I. R. McNab, R. C. Shiell, and F. E. Smith, Phys. Chem. Chem. Phys. **5**, 663 (2003).
[5] D. Mathur, Phys. Rep. **391**, 1 (2004).
[6] F. Penent, R. I. Hall, R. Panajotović, J. H. D. Eland, G. Chaplier, and P. Lablanquie, Phys. Rev. Lett. **81**, 3619 (1998).
[7] M. Lundqvist, P. Baltzer, D. Edvardsson, L. Karlsson, and B. Wannberg, Phys. Rev. Lett. **75**, 1058 (1995).
[8] L. H. Andersen, J. H. Posthumus, O. Vahtras, H. Ågren, N. Elander, A. Nunez, A. Scrinzi, M. Natiello, and M. Larsson, Phys. Rev. Lett. **71**, 1812 (1993).
[9] J. P. Bouhnik, I. Gertner, B. Rosner, Z. Amitay, O. Heber, D. Zajfman, E. Y. Sidky, and I. Ben-Itzhak, Phys. Rev. A **63**, 032509 (2001).
[10] T. A. Field and J. H. D. Eland, Chem. Phys. Lett. **211**, 436 (1993).
[11] M. Hochlaf, R. I. Hall, F. Penent, H. Kjeldsen, P. Lablanquie, M. Lavollée, and J. H. D. Eland, Chem. Phys. **207**, 159 (1996).
[12] G. Dawber, A. G. McConkey, L. Avaldi, M. A. MacDonald, G. C. King, and R. I. Hall, J. Phys. B **27**, 2191 (1994).
[13] J. H. D. Eland, Chem. Phys. **294**, 171 (2003).
[14] O. Furuhashi, T. Kinugawa, S. Masuda, C. Yamada, and S. Ohtani, Chem. Phys. Lett. **337**, 97 (2001).
[15] M. Larsson, G. Sundström, L. Broström, and S. Mannervik, J. Chem. Phys. **97**, 1750 (1992).
[16] F. R. Bennett and I. R. McNab, Chem. Phys. Lett. **251**, 405 (1996).
[17] D. Cossart and J. M. Robbe, Chem. Phys. Lett. **311**, 248 (1999).
[18] R. W. Wetmore, R. J. LeRoy, and R. K. Boyd, J. Phys. Chem. **88**, 6318 (1984).
[19] M. Larsson, B. J. Olsson, and P. Sigray, Chem. Phys. **139**, 457 (1989).
[20] J. H. D. Eland, M. Hochlaf, G. C. King, P. S. Kreynin, R. J. LeRoy, I. R. McNab, and J. M. Robbe, J. Phys. B **37**, 3197 (2004).
[21] L. Veseth, J. Phys. B **34**, L773 (2001).
[22] O. Vahtras, H. Ågren, P. Jörgensen, H. J. A. Jensen, T. Helgaker, and J. Olsen, J. Chem. Phys. **96**, 2118 (1992).
[23] E. Y. Sidky and I. Ben-Itzhak, Phys. Rev. A **60**, 3586 (1999).
[24] A. U. Hazi and H. S. Taylor, Phys. Rev. A **1**, 1190 (1970).
[25] R. Lefebvre, J. Phys. Chem. **89**, 4201 (1985).
[26] A. Mandelshtam, H. S. Taylor, V. Ryaboy, and N. Moiseyev, Phys. Rev. A **50**, 2764 (1994).
[27] N. Moiseyev, Phys. Rep. **302**, 211 (1998).
[28] V. Ryaboy and N. Moiseyev, J. Chem. Phys. **103**, 4061 (1995).
[29] V. Špirko, P. Piecuch, and O. Bludský, J. Chem. Phys. **112**, 189 (2000).
[30] F. Mrugała, P. Piecuch, V. Špirko, and O. Bludský, J. Mol. Struct. **555**, 43 (2000).
[31] R. Burcl, P. Piecuch, V. Špirko, and O. Bludský, J. Mol. Struct.: THEOCHEM **591**, 151 (2001).
[32] Y. Li, O. Bludský, G. Hirsch, and R. J. Buenker, J. Chem. Phys. **107**, 3014 (1997).
[33] H.-J. Werner, P. J. Knowles, R. Lindh *et al.*, MOLPRO, Version 2002.6, a package of ab initio programs, 2003; see http://www.molpro.net
[34] T. H. Dunning, Jr., J. Chem. Phys. **90**, 1007 (1989).
[35] H.-J. Werner and P. J. Knowles, J. Chem. Phys. **89**, 5803 (1988).
[36] P. J. Knowles and H.-J. Werner, Chem. Phys. Lett. **145**, 514 (1988).
[37] S. R. Langhoff and E. R. Davidson, Int. J. Quantum Chem. **8**, 61 (1974).
[38] K. Raghavachari, G. W. Trucks, J. A. Pople, and M. Head-Gordon, Chem. Phys. Lett. **157**, 479 (1989).
[39] P. J. Knowles, C. Hampel, and H.-J. Werner, J. Chem. Phys. **99**, 5219 (1993).
[40] W. E. Milne, Phys. Rev. **35**, 863 (1930).
[41] See EPAPS Document No. E-JCPSA6-124-008618 for the results comprising a complete set of the spectroscopic constants of the probed electronic states and details illustrating the stabilization and complex-scaling procedures used in the present study. This document can be reached via a direct link in the online article's HTML reference section or via the EPAPS homepage (http://www.aip.org/pubservs/epaps.html).
[42] B. R. Johnson, J. Chem. Phys. **69**, 4678 (1978).
[43] H. Lefebvre-Brion and R. W. Field, *Pertubations in the Spectra of Diatomic Molecules* (Academic, New York, 1986).

Downloaded 04 Jun 2006 to 130.183.82.42. Redistribution subject to AIP license or copyright, see http://jcp.aip.org/jcp/copyright.jsp

TABLE A. Spectroscopic constants for low-lying electronic states of CO^{2+}.

State	Reference or basis set	R_e (Å)	ω_e (cm^{-1})	$\omega_e x_e$ (cm^{-1})	B_e (cm^{-1})	α_e (cm^{-1})
$X^3\Pi$	Eland *et al.*[11]	1.2479	1435.2	24.6	1.579	0.028
	icMRCI/V6Z/AE[a]	1.2392	1480.3	23.2	1.599	0.026
	RCCSD(T)/V6Z/AE[a]	1.2377	1480.2	17.3	1.600	0.022
$a^1\Sigma^+$	Eland *et al.*[11]	1.1592	1920.5	16.7	1.829	0.021
	icMRCI/V6Z/AE[a]	1.1548	1951.3	17.6	1.844	0.021
	RCCSD(T)/V6Z/AE[a]	1.1535	2002.3	31.7	1.853	0.026
$A^3\Sigma^+$	Eland *et al.*[11]	1.1348	2043.8	16.3	1.909	0.022
	icMRCI/V6Z/AE[a]	1.1310	2068.6	20.3	1.919	0.019
$b^1\Pi$	Eland *et al.*[11]	1.2500	1487.7	17.2	1.573	0.023
	icMRCI/V6Z/AE[a]	1.2430	1517.5	17.3	1.591	0.023
$c^1\Delta$	Eland *et al.*[11]	1.7076	545.9	38.9	0.843	0.048
	icMRCI/V6Z/AE[a]	1.7019	556.8	7.5	0.848	0.013
$d^1\Sigma^+$[b]	Eland *et al.*[11]	1.5497	1125.6	7.6	1.023	−0.012
	icMRCI/V6Z/AE[a]	1.5475	1099.3	3.7	1.028	−0.008
$e^1\Sigma^+$	icMRCI/V6Z/AE[a]	1.2546	3294.2	139.4	1.562	−0.001

[a]All electrons correlated in the CASSCF/icMRCI or RCCSD(T) calculations of the PEF's.

[b]Spectroscopic constants for the outer potential well. The lowest three vibrational levels corresponding to the inner potential well are located at 1195.9, 3546.4 and 5840.4 cm^{-1}, relative to the energy of this minimum at $R_e = 1.0838$ Å. The corresponding rotational constants are $B_e = 2.130$ and $\alpha = 0.090\,cm^{-1}$.

Supplementary Material

The adiabatic potential energy ($V(x)$) and spin-orbit coupling ($C(x)$) functions used in the complex-scaling calculations were fitted to the following (analytical) forms.

$$V(x) = \frac{\left(\sum_{i=0}^{M} V_i (x+c)^i\right)^2}{\sum_{i=0}^{P} w_i (x+c)^i} \cdot \left(e^{-\alpha(x+c)}\right)^s + \frac{\sum_{i=0}^{L} a_i (x+c)^i}{\sum_{i=0}^{N} b_i (x+c)^i} + \sum_{i=0}^{K} d_i (x+c)^i \tag{1}$$

and

$$C(x) = \left(\sum_{i=0}^{M} V_i x^i\right)^s e^{-\alpha x} + \frac{\sum_{i=0}^{L} a_i x^i}{\sum_{i=0}^{N} b_i x^i} + \sum_{i=0}^{K} d_i x^i. \tag{2}$$

The parameters resulting from the fitting procedure are collected in Tables B and C.

TABLE B. The fitting parameters of the potential energy functions of the four lowest electronic states of CO^{2+}.

Parameters	$X^3\Pi$	$^3\Sigma^-$	$a^1\Sigma^+$	$b^1\Pi$
V_0	0	+16417.6	−121.37	−118.669
V_1	237.3	−23311.2	157.499	346.763
V_2	−35.2	18041.8	0	−105.563
V_3	0	−6583.8	72.5883	30.0472
V_4	0	968.9	−46.8758	−4.4042
V_5	0.1548	0	6.1017	0.3895
V_6	−0.0894	0	1.2028	−0.0145
α	0.6815	2.9401	1.2974	0.4230
c	−2.3556	0	−1.4985	−2.0272
s	2	1	2	2
w_0	0	0	0.1082	0
w_1	0	0	−0.0714	0
w_2	0	0	0.0130	0
a_0	−575.73	0	0	0
a_1	9875.81	0	0	86499.9
b_0	5.5529	0	0	8.1569
b_1	−7.6229	0	0	0
b_2	8.4295	0	0	13.0595
b_3	−6.1586	0	0	−10.4752
b_4	2.2343	0	0	2.7033
d_0	0	3105.01	996.0	911.5
d_2	−260.60	−6538.54	0	0
d_3	−98.74	2935.67	0	0
d_4	9.7616	−523.416	57.8034	0
d_5	0	41.6482	−12.7328	0
d_6	0	−1.2360	0.7135	0

TABLE C. The fitting parameters of the spin-orbit coupling functions of the four lowest electronic states of CO^{2+}.

Parameters	$^3\Pi$ $^3\Sigma^-$	$^3\Pi$ $^1\Sigma^+$	$^3\Pi$ $^1\Pi$	$^3\Sigma^-$ $^1\Sigma^+$	$^3\Sigma^-$ $^1\Pi$
V_0	0	1.5370	6.8361	3.1672	0
V_1	0.6731	0	−5.5510	−1.6037	−6.9383
V_2	0.2328	0.3478	2.1158	1.0142	2.9955
α	27.6174	23.1823	24.3841	45.1291	43.0308
s	60.2194	47.8256	34.0115	61.9735	57.5256
a_0	0	0	3.1285	0	0
a_1	1.9299	0	−1.2582	0	46.2716
a_2	−0.4549	0	0.1376	0	−10.4941
b_0	0.7616	0	0.0571	0	30.3209
b_1	−0.5016	0	−0.0271	0	−13.4572
b_2	0.0909	0	0.0039	0	1.5623
d_0	−3.7379	−488.0300	0	0	−40.9433
d_1	0.2241	277.2310	−2.3601	0	40.1572
d_2	0	−58.7743	0	0	−9.7707
d_3	0	5.4547	0	0	0.9674
d_4	0	−0.1862	0	0	−0.0341

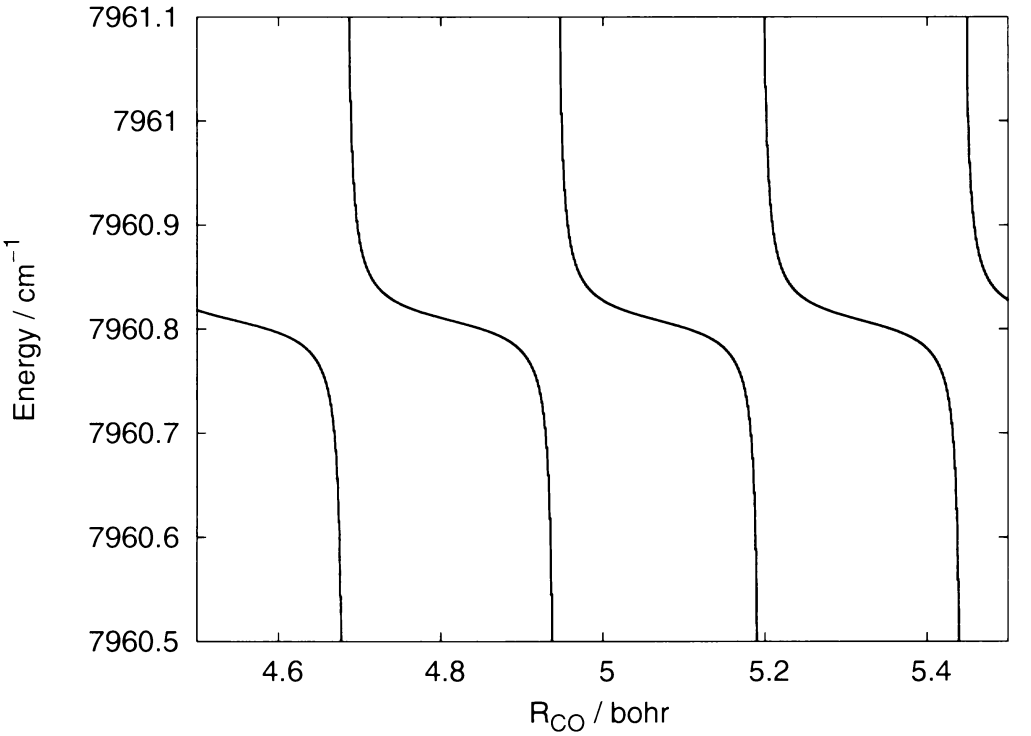

FIG. A: A part of the global stabilization diagram of CO^{2+} pertaining to the quasi-bound $v = 2$, $b^1\Pi$ state.

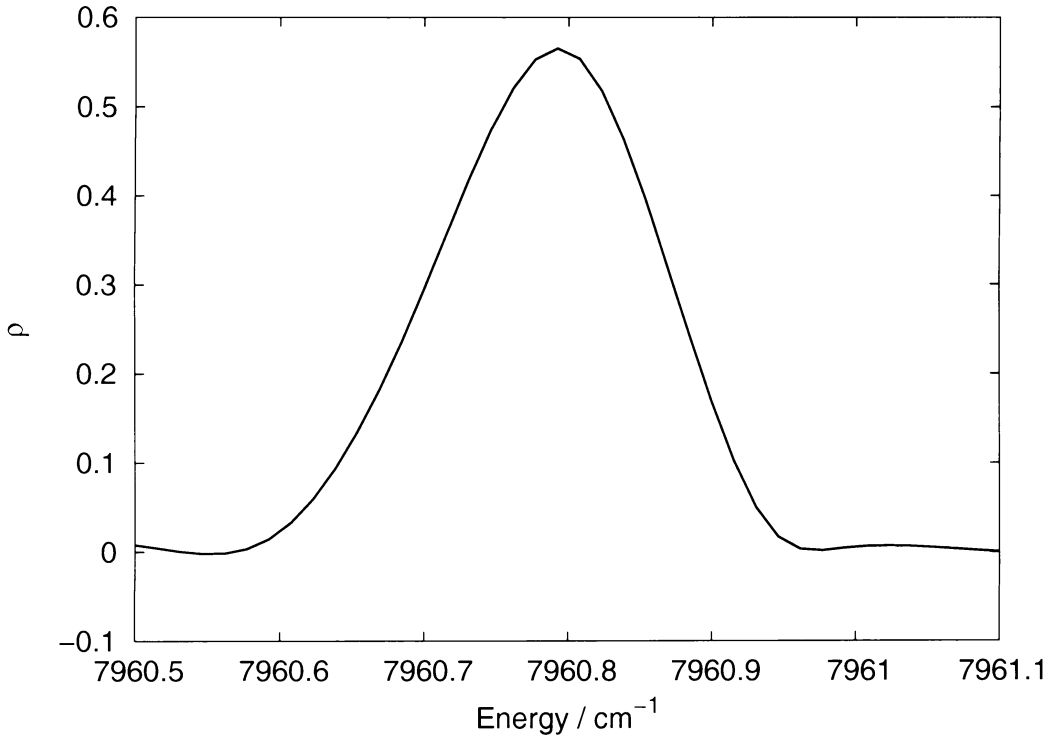

FIG. B: The density of states of CO^{2+} obtained from the stabilization diagram plotted in Fig. A

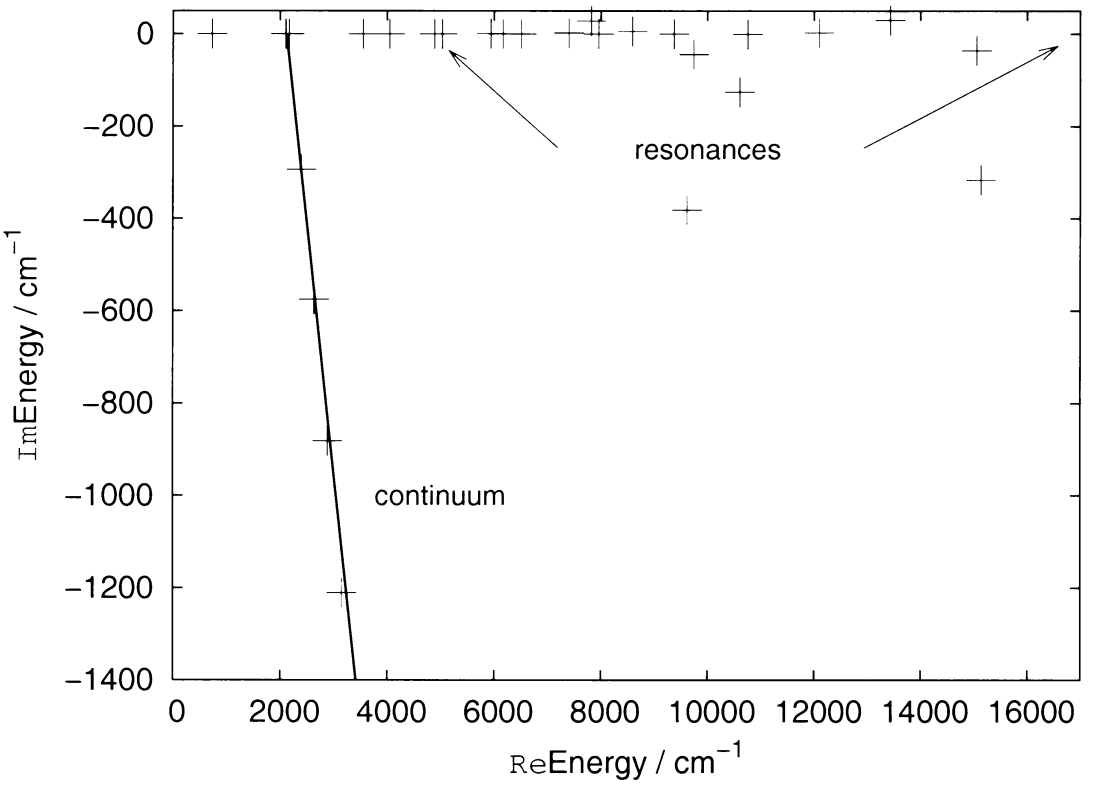

FIG. C: $\theta = 0.06$ rad energy spectrum of the complex-scaled Hamiltonian of CO^{2+}.

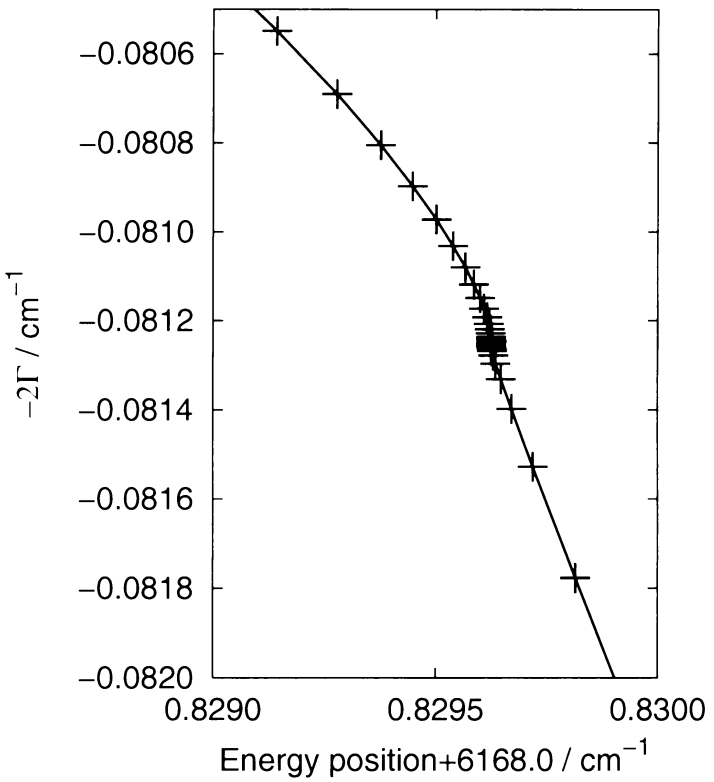

FIG. D: θ trajectory for $v = 4$. $X^3\Pi$ CO^{2+}. θ changed from 0.0001 to 0.06 rad. The stationary point is located in the middle of the figure.

Theoretical study of the CS^{2+} dication

T. Šedivcová and V. Špirko[a]
Department of Molecular Modeling, Academy of Sciences of the Czech Republic, Flemingovo nam. 2, 166 10 Prague 6, Czech Republic; Center for Biomolecules and Complex Molecular Systems, Academy of Sciences of the Czech Republic, Flemingovo nam. 2, 166 10 Prague 6, Czech Republic; and Institute of Organic Chemistry and Biochemistry, Academy of Sciences of the Czech Republic, Flemingovo nam. 2, 166 10 Prague 6, Czech Republic

J. Fišer
Department of Physical and Macromolecular Chemistry, Faculty of Science, Charles University, Hlavova 2030, 128 40 Prague 2, Czech Republic

(Received 25 July 2006; accepted 7 September 2006; published online 24 October 2006)

The potential energy and spin-orbit coupling functions of 11 lowest electronic states of CS^{2+} dication have been calculated using internally contracted multireference configuration method. Using these functions, the positions and widths of the corresponding vibronic levels have been evaluated by means of the stabilization and log-phase-amplitude methods. The states governing the second step in the sequential pathway $CS_2^{3+} \rightarrow S^+ + CS^{2+} \rightarrow S^+ + C^+ + S^+$ of the overall three-body Coulomb explosion of CS_2^{3+} have been determined. © *2006 American Institute of Physics.*
[DOI: 10.1063/1.2358982]

I. INTRODUCTION

A growing interest in both the experimental and theoretical studies of multiply charged molecular ions in the last two decades has been stimulated by their unusual bonding and other physicochemical properties in which they differ from single-charged ions and also by the importance of their role in both plasma and ionosphere chemistry and astrophysics.[1-5] The characteristic shape of the majority of the potential energy curves of the molecular dications, i.e., a local potential minimum separated from the lower dissociation limit by a broad barrier, may be viewed as the balance between the chemical bonding of charged ions and their Coulomb repulsion.

Hishikawa *et al.*[6,7] have recently studied three-body Coulomb explosion decays of CS_2 in intense laser fields by triple coincidence momentum imaging of the fragment ions. They demonstrated that fragmentation of the CS_2^{3+} parent ion proceeds concertedly, $CS_2^{3+} \rightarrow S^+ + C^+ + S^+$, or sequentially as a two-step process, $CS_2^{3+} \rightarrow S^+ + CS^{2+} \rightarrow S^+ + C^+ + S^+$. While the metastable triatomic dication CS_2^{2+} has been the subject of considerable efforts, both experimental[8,9] and theoretical,[10,11] much less is known about CS^{2+}. Krishnamurthi *et al.*[12] have studied charge stripping of CS^+ and dissociation of CS^{2+} by means of the ion translational energy spectrometry. The CS^{2+} dications were generated by electron double ionization of either CS or by dissociative double ionization of CS_2. These measurements were accompanied by calculations of the potential energy functions (PEFs) of the two lowest electronic states ($X\,^3\Pi$ and $^1\Sigma^+$) of CS^{2+} using the QCISD/6-311G* method. These theoretical calculations are undoubtedly too limited to provide a sufficiently complete theoretical rationalization of the observed data. To overcome this problem, we decided to perform the theoretical calculations for a much larger set of the pertinent electronic states. Apart from the potential energy functions, we have also evaluated all relevant spin-orbit coupling functions. In turn, to allow comparison with experiment, the calculated functions were used to calculate (i) the spectroscopic constants for strongly metastable vibronic states, (ii) the first ionization energy of CS^+, double ionization energy and kinetic energy release (KER) upon dissociation of CS^{2+}, and (iii) the spin-orbit induced and tunneling lifetimes for some selected vibronic metastable levels.

The actual calculations were performed at the same level of accuracy as in the case of our recent study on the isovalent CO^{2+} species.[13] As the characteristics calculated in that study were found to be in very good agreement with the experimental data, we believe that the present CS^{2+} data are capable of serving for a physically correct description of the studied states, particularly of the states governing the sequential pathway of the overall three-body Coulomb explosion of CS_2^{3+}.

II. METHODS AND COMPUTATIONAL DETAILS

The PEFs were calculated using the internally contracted multireference configuration interaction (icMRCI) method[14,15] enabling a proper accounting for the strong multiconfiguration effects in the whole region of internuclear distances for the ground and excited electronic states. The orbitals for the CI treatment of CS, CS^+, and CS^{2+} were obtained in state-averaged complete-active-space self-consistent field (CASSCF) calculations with equal weights for the participating states of the same spin multiplicity. The full valence space consisted of the 5σ-8σ, 2π, and 3π orbitals. The core molecular orbitals ($4\times a_1$, $1\times b_1$, and $1\times b_2$ in C_{2v} symmetry) were constrained to be doubly occupied in all electron configurations but fully optimized. The icMRCI

[a]Electronic mail: spirko@marge.uochb.ca

 © 2006 American Institute of Physics

Downloaded 26 Oct 2006 to 130.183.82.42. Redistribution subject to AIP license or copyright, see http://jcp.aip.org/jcp/copyright.jsp

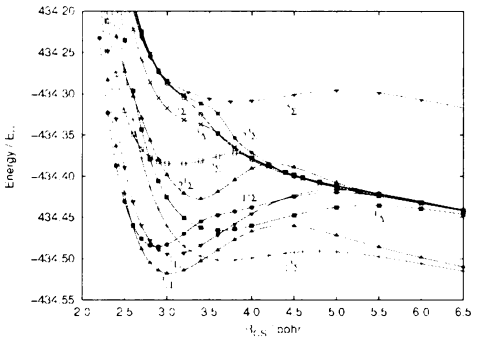

FIG. 1. The icMRCI potential energy functions of the 11 lowest electronic states of the CS^{2+} dication.

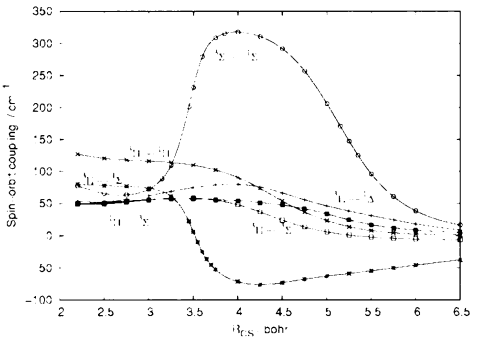

FIG. 2. The spin-orbit couplings between the five lowest electronic states of the CS^{2+} dication.

method including the Davidson correction (icMRCI+Q) was also used. Single and double ionization energies of CS were calculated using the spin-restricted coupled cluster method with singles, doubles, and a perturbative estimate of triple excitations[16,17] [RCCSD(T)] and also using the multireference version of the averaged coupled pair functional (MR-ACPF) method.[18] The correlation-consistent cc-pV5Z basis set of Dunning and co-workers[19,20] was used. All the CASSCF, icMRCI, RCCSD(T), and MR-ACPF calculations were performed using the MOLPRO 2002 suite of programs.[21] The spin-orbit integrals were evaluated with the icMRCI wave functions using the Breit-Pauli operator, as implemented in the MOLPRO code. Due to the limitations of this program, only the *spdf* orbital subset of the cc-pV5Z basis set was employed in the calculations.

The spectroscopic constants of the strongly metastable states have been derived from the rovibronic energies obtained numerically from the respective PEFs using the Numerov-Cooley integration procedure.[22] The tunneling lifetimes of these states have been evaluated using the log-phase-amplitude method of Sidky and Ben-Itzhak.[23]

The widths Γ_{res} and energies E_{res} of the quasibound (resonance) states have been calculated using the stabilization method[24–26] within the framework of a multichannel Schrödinger analysis. The actual implementation of this approach consists of a repeated diagonalization of the system Hamiltonian $\mathbf{H}^d$ in a series of enclosing boxes with their box size R varying

$$R_0 < R < R_0 + \Delta R.$$

The primary result of this calculation are functional dependences of the resulting eigenvalues $E(R)$ (the so-called stabilization diagram), which in turn provide average densities of states $\rho(E)$, from which the resonance energies and widths can be determined by the Lorentzian fitting (for details see Ref. 13). The Hamiltonian $\mathbf{H}^d$ used in this approach is represented by the following set of coupled Schrödinger equations:

$$\mathbf{H}^d = -\frac{\hbar^2}{2\mu}\frac{d^2}{dR^2}\mathbf{I} + \mathbf{V}^d(R), \tag{1}$$

where $V_{ii}^d(R)$ are the adiabatic *ab initio* potentials, $V_{ij}^d(R)$ are the spin-orbit interactions, and I and μ are the unit matrix and reduced mass, respectively.

III. RESULTS AND DISCUSSION

To probe the accuracy of the used *ab initio* theory, this very same method, CAS, and the basis set were also used for the evaluation of the spectroscopic constants of the parent CS^+ and CS molecules. A comparison of these constants with their available experimental[27,28] and theoretical[29,30] counterparts shows a very good agreement for all data (the differences between our R_e's and ω_e's and the corresponding experimental data are at most 0.006 Å and 6 cm^{-1}, respectively).

The adiabatic PEFs of the 11 lowest electronic states of CS^{2+} and the pertinent spin-orbit couplings between the five lowest states are displayed in Figs. 1 and 2, respectively. The ordering of the quasibound states is $X\,^3\Pi$, $A\,^3\Sigma^-$, $a\,^1\Pi$, $b\,^1\Sigma^+$, $c\,^1\Delta$, $d\,^1\Sigma^+$, $B\,^3\Sigma^+$,.... A comparison with the ordering for the isovalent CO^{2+} species, $X\,^3\Pi$, $a\,^1\Sigma^+$, $b\,^1\Pi$, $c\,^1\Delta$, $A\,^3\Sigma^+$, $d\,^1\Sigma^+$, $e\,^1\Sigma^+$,...,[13,31] reveals that the ordering of the lowest $^1\Pi$ and $^1\Sigma^+$ states (and also $d\,^1\Sigma^+$ and $^3\Sigma^+$ states) in the two dications is reversed. Unlike in CO^{2+}, where the $^3\Sigma^-$ state is purely repulsive, in CS^{2+} it is a weak quasibound state with a very broad and low barrier ($E_b \sim 0.26$ eV).

Like in the case of CO^{2+}, the predissociation paths of CS^{2+} are strongly affected by the spin-orbit couplings. The decisive importance of these effects is shown in Fig. 3. The figure displays four *double adiabatic* potentials which were obtained as the lowest eigenvalues of the full coupled channel energy matrix possessing the adiabatic PEFs on its diagonal and the spin-orbit couplings forming its off-diagonal part.

As arises from Fig. 1, the $X\,^3\Pi$ and $A\,^3\Sigma^-$ are the only

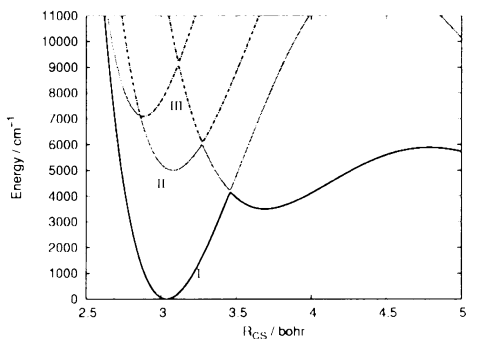

FIG. 3. The *double adiabatic* potential energy curves for the lowest electronic states of the CS^{2+} dication.

Downloaded 26 Oct 2006 to 130.183.82.42. Redistribution subject to AIP license or copyright, see http://jcp.aip.org/jcp/copyright.jsp

TABLE I. Dominant electronic configurations, icMRCI excitation energies T_0 including zero point vibrational corrections, and spectroscopic constants for the low-lying quasibound electronic states of CS^{2+}.

State	Dominant configuration	T_0 (eV)	R_e (Å)	ω_e (cm^{-1})	$\omega_e x_e$ (cm^{-1})	B_e (cm^{-1})	α_e (cm^{-1})
$X\,^3\Pi$	$5\sigma^2 6\sigma^2 2\pi^3 7\sigma^1$	0	1.607	1032.6	10.6	0.748	0.008
$A\,^3\Sigma^-$	$5\sigma^2 6\sigma^2 7\sigma^2 2\pi^2$	0.385	1.953	515.8	13.8	0.505	0.008
$a\,^1\Pi$	$5\sigma^2 6\sigma^2 2\pi^3 7\sigma^1$	0.624	1.629	975.3	9.6	0.728	0.008
$b\,^1\Sigma^+$	$5\sigma^2 6\sigma^2 2\pi^4$	0.874	1.525	1170.5	22.4	0.825	0.002
$c\,^1\Delta$	$5\sigma^2 6\sigma^2 7\sigma^2 2\pi^2$	1.374	1.919	575.0	5.8	0.524	0.007
$d\,^1\Sigma^+$	$5\sigma^2 6\sigma^2 7\sigma^2 2\pi^2$	2.440	1.791	1118.2	19.8	0.604	0.000
$B\,^3\Sigma^+$	$5\sigma^2 6\sigma^2 2\pi^3 3\pi^1$	3.570	1.651	591.7	6.4	0.718	0.018
$^3\Delta$	$5\sigma^2 6\sigma^2 2\pi^3 3\pi^1$	[a]					
$^1\Sigma^-$	$5\sigma^2 6\sigma^2 7\sigma^2 2\pi^3 3\pi^1$	[a]					
$2\,^3\Sigma^-$	$5\sigma^2 6\sigma^2 2\pi^3 3\pi^1$	[a]					
$^5\Sigma^-$	$5\sigma^2 6\sigma^2 2\pi^2 3\pi^2$	5.620	2.021	439.2	8.8	0.473	0.002

[a]Repulsive state.

ıtes dissociating to the lowest asymptote $C^+(^2P_u)$ $S^+(^4S_u)$. The PEFs for the first two excited singlet states, $^1\Pi$ and $b\,^1\Sigma^+$, pertain to the second asymptote $C^+(^2P_u)$ $S^+(^2D_u)$. The $d\,^1\Sigma^+$ state dissociates to the third asymptotic nit $C^+(^2P_u)+S^+(^2P_u)$, whereas the quintet state into the $^4P_g)+S^+(^4S_u)$ state, in accordance with the Wigner-itmer correlation rules. The asymptotic electronic energies CS^{2+} were calculated at the longest accessible bond sepa-ion (e.g., $R=250$ bohrs). Each potential was then extrapo-ed to infinity using an assumed $1/R$ functional form. The lculated differences between the individual asymptotic nits were found in a reasonable agreement with the atomic ectroscopic data,[32] providing thus evidence for the reliabil- of the calculated potentials.

The dominant electronic configurations, icMRCI excita-n energies, and the spectroscopic constants of the calcu-ed electronic states of CS^{2+} are given in Table I. There are experimental data to compare with. It should be noted, wever, that the harmonic frequencies for the $X\,^3\Pi$ and Σ^+ states (1083 and 1240 cm^{-1}) calculated within the CISD(T)/6-311G* model[12] are not significantly different m our values. Moreover, the earlier R_e's, 1.6 and 1.52 Å,[12] both of the states mentioned above are also very close to r icMRCI results.

Another probing of theory consisted in using the CSD(T), ACPF, icMRCI, and icMRCI+Q methods to aluate the vertical ionization energies of the parent mol-ıles. For the first ionization energy of neutral CS, we have tained 11.31, 11.22, 11.14, and 11.23 eV, respectively, as mpared to the experimental values of 11.33 (Refs. 27 and) and 11.319±0.006 eV.[34] The vertical ionization energy of CS^+, calculated to be 21.63, 21.57, 21.48, and 21.58 eV, and the vertical double ionization energy of CS to the $X\,^3\Pi$ state of CS^{2+}, 32.79, 32.65, 32.38, and 32.67 eV, are also in a very good agreement with the respective values of 22.0±0.9 and 33.3±1.1 eV provided by the ion translational energy spectrometry.[12]

The last quantity which was probed in this study and which may provide important information on the ion decay mechanism is the KER upon unimolecular dissociation. Krishnamurthi *et al.*[12] measured this quantity in the 6 keV collisions of CS^{2+} with N_2, $CS^{2+}+N_2 \rightarrow C^++S^++N_2+T_{c.m.}$, where $T_{c.m.}$ corresponds to the kinetic energy released in the center-of-mass frame and obtained 5.20±0.01 and 2.80±0.01 eV. Hishikawa *et al.*[6] derived for KER the value of 5.3(6) eV at step II ($CS^{2+} \rightarrow C^++S^+$) of the sequential three body Coulomb explosion of CS_2^{3+}. In our calculations, KER was evaluated for the $X\,^3\Pi$, $A\,^3\Sigma^-$, $a\,^1\Pi$, and $b\,^1\Sigma^+$ states using three methods: ACPF, icMRCI, and icMRCI +Q. Due to the crossing with the nearly repulsive $A\,^3\Sigma^-$ state and the large magnitude of the corresponding spin-orbit coupling (see Fig. 3), both aforementioned singlet $a\,^1\Pi$ and $b\,^1\Sigma^+$ states were assumed to dissociate to the lowest asymptotic limit. Using the icMRCI method, the KER ($v=0$) values of the listed electronic states method were determined to be 3.92, 4.32, 4.55, and 4.80 eV, respectively. The results obtained by the ACPF and icMRCI+Q methods deviate from these data at most by 0.04 eV. We have also made an estimate of KER($X\,^3\Pi, v>0$) based on the thermochemical cycle by combining measurements of the first ionization energies of C and S [11.26 and 10.36 eV (Ref. 32)], the dissociation energy of CS [D_0=7.354 eV (Ref. 30)], and

TABLE II. Tunneling lifetimes (in seconds) for four lowest electronic states of CS^{2+}.

v	$X\,^3\Pi$	v	$A\,^3\Sigma^-$	v	$a\,^1\Pi$	v	$b\,^1\Sigma^+$
10	4.7×10^{4}	0	2.2×10^{7}	18	2.2×10^{6}	15	7.1×10^{4}
11	1.8	1	1.7×10^{2}	19	62	16	7.5
12	1.9×10^{-4}	2	5.4×10^{-3}	20	4.2×10^{-3}	17	1.6×10^{-3}
13	5.0×10^{-8}	3	5.6×10^{-7}	21	7.2×10^{-7}	18	6.9×10^{-7}
14	3.9×10^{-11}	4	2.0×10^{-10}	22	3.3×10^{-10}	19	7.1×10^{-10}
15	2.1×10^{-13}	5	5.1×10^{-13}	23	7.2×10^{-13}	20	2.3×10^{-12}

ownloaded 26 Oct 2006 to 130.183.82.42. Redistribution subject to AIP license or copyright, see http://jcp.aip.org/jcp/copyright.jsp

TABLE III. Vibrationally averaged spin-orbit coupling constants A_v of CS^{2+} ($X\,^3\Pi$), in cm^{-1}.

v	A_v	v	A_v	v	A_v	v	A_v	v	A_v	v	A_v	v	A_v	v	A_v
0	140.68	1	140.24	2	140.03	3	139.59	4	139.15	5	138.49	6	137.61	7	136.51

e vertical double ionization energy CS [33.3 eV (Ref. 12)]; e resulting KER is 4.33 eV. Since the experimental double nization energy is associated with rather high error bars, it not surprising that a similar estimate stemming from the CCSD(T) adiabatic double ionization energy (32.76 eV) ields a significantly lower value of KER($X\,^3\Pi, v=0$) 3.78 eV, which is close to the icMRCI value (3.92 eV) lculated directly. Interestingly, if we take KER released om the $v=13$ vibrational level having the tunneling lifetime $\cdot 5\times 10^{-8}$ s (see Table II), we obtain KER($X\,^3\Pi, v=13$) $\cdot$5.29 eV, in accordance with the experimental values.

As can be seen in Fig. 2, the most striking feature of the in-orbit interactions is the R dependence of the coupling etween the $^3\Sigma^-$ and $^1\Sigma^+$ states. The vibrational dependence f the remaining couplings is much less profound, which is flected by only a moderate vibrational dependence of the in-orbit constants of the ground electronic state $X\,^3\Pi$ (see able III). The shapes of the calculated couplings coincide osely with the shapes of their CO^{2+} counterparts calculated our recent study.[13] Worthy to be noted, the CS^{2+} couplings not coincide so closely with the CO^{2+} couplings obtained Andersen *et al.*[35] by means of the multiconfigurational near response approach. The reasons causing this dishar- ony, especially strong in the case of the $^3\Pi$-$^3\Sigma^-$ coupling, e unclear and their clarification would require a deeper eoretical analysis.

The actual calculations of the vibronic energies and their widths were performed with the Hamiltonian (1) including the five lowest electronic states with R varying from 2.2 to 9.9 bohrs. The eigenvalue problem for this Hamiltonian was solved using the renormalized Numerov method.[36] Besides these numerically exact calculations, also an approximate double diabatic modeling was probed. This approach is based on unitary transformations of the original Hamiltonian (performed separately for each value of R) which diagonalize the potential energy matrices $\mathbf{V}^d$ while neglecting the off-diagonal (nonadiabatic) terms induced by these transformations.

The resonance energies, widths (in cm^{-1}), and lifetimes (in μs) determined from the actual calculations are collected in Table IV. It is evident from the table that the characteristics obtained by means of the adiabatic [one-dimensional (1D)] calculations are only crude approximates of their genuine values and, with the exception of strongly metastable states, they become highly inaccurate. This is reflected especially by the energy widths, which achieve reliable values only for the lowest adiabatic state. In other words, the spin-orbit interaction causes heavy mixing of the adiabatic molecular states and prevents their simple assignment in terms of either "spin-orbit free" or "double adiabatic" quantum numbers. Nevertheless, the double adiabatic picture is not completely useless, as it provides simple qualitative insight

TABLE IV. Energy positions (cm^{-1}) calculated using one dimensional (1D) and five dimensional (stabilization method) approach and lifetimes τ (μs) of the lowest vibronic resonances of CS^{2+}.

State	v	1D	Γ (cm^{-1})	Stabilization method	Γ (cm^{-1})	τ (μs)
I	0	509.9		509.87	e	
	1	1521.4		1521.43	e	
	2	2507.9		2509.19	e	
	3	3450.4		3473.57	e	
	4	3760.9		3754.82	e	
	5	4100.5		4239.61	e	
	6	4461.5		4414.81	e	
	7	4814.6		4695.77	e	
	8	5190.4	3.8×10^{-5}	5331.68	4.7×10^{-5}	0.11
	9	5504.5	2.8×10^{-2}	5494.92	1.2×10^{-2}	4.5×10^{-4}
	10	5780.0	5.23	5808.37	8.55	6.2×10^{-7}
				6445.75	2.87	1.9×10^{-6}
II	0	5114.9		5114.90	6.9×10^{-6}	0.77
	1	5497.1		5486.01	5.2×10^{-3}	1.0×10^{-3}
				5488.54	3.4×10^{-1}	1.6×10^{-5}
	2	6279.0		6221.62	1.93	2.8×10^{-6}
	3	6824.0		7383.37	0.56	9.5×10^{-6}
	4	7538.2				
	5	8144.3				
	6	8785.9				
III	0	7138.2		7084.65	1.10	4.8×10^{-6}
	1	7870.0		7683.74	3.36×10^{-2}	1.5×10^{-4}
	2	8596.5				

Downloaded 26 Oct 2006 to 130.183.82.42. Redistribution subject to AIP license or copyright, see http://jcp.aip.org/jcp/copyright.jsp

into the behavior of individual vibronic states: the states which can be classified as low-lying states in the adiabatic approximation exhibit fairly high stability while the only states that undergo fast decays are those containing energies which are comparable to the dissociation limits.

Relying on the calculated patterns of the vibronic energy levels and their lifetimes, obviously, one can easily propose all possible decay mechanisms of the CS^{2+} molecular states pertaining to its four lowest electronic states, and, if knowing the initial populations of these states, even derive rates for these decays. The calculated characteristics may also be of some help in the situations when these populations are unavailable and difficult to estimate, for instance, in the prominent case of the Coulomb explosions. As noted in Introduction, in studying the Coulomb explosion of CS_2 in intense laser fields, Hishikawa *et al.*[6,7] have given evidence that intermediate CS^{2+} ions are formed in the first step of the sequential fragmentation of the CS_2^{3+} ions. Using coincidence momentum measurements, they determined a trajectory originating from the rotational motion of the CS^{2+} dications and by fixing its internuclear distance at the equilibrium ground state *ab initio* value,[12] they estimated the rotational period $\tau_{rot} \sim 20$ ps for $J=1$. Relying on this value, they deduced that the lifetime of the metastable CS^{2+} could be bracketed as $10\ \text{ps} < \tau \ll 1\ \mu\text{s}$. Finally, by assuming that CS^{2+} is mostly prepared in the $X\,^3\Pi$ state and using the WKB estimate for the lifetime of CS^{2+} in this state, they arrived at a conclusion that the *ab initio* potential[12] needs to be lowered, rather unreasonably, by ~ 1.0 eV to account for the observation. According to our results, the lowest $X\,^3\Pi$ state is heavily mixed with the firstly excited $^3\Sigma^-$ state, which possesses a much lower dissociation asymptote (see Fig. 3). Both the mixed states thus possess resonance states satisfying the experimental constraints (see Table IV) without any need of amending *ab initio* theory.

IV. CONCLUSION

The CASSCF/icMRCI wave functions were used to calculate the potential energy and spin-orbit coupling functions of the lowest electronic states of CS^{2+}. The positions and widths/lifetimes of the metastable vibrational states of the four lowest electronic states coupled by the spin-orbit interaction were obtained using the stabilization and log-phase-amplitude methods. The calculated lifetimes strongly evidence the predominance of the spin-orbit induced predissociation in the decay processes of CS^{2+}, particularly in the sequential three-body Coulomb explosion of CS^2 in intense laser fields.

ACKNOWLEDGMENTS

The authors wish to thank METACenter (http://meta.cesnet.cz) for time allocation. This study was supported by the Grant Agency of the Academy of Sciences of the Czech Republic (Grant Nos. A400550511, 1ET400400410, and KJB100550501), by the Grant Agency of the Czech Republic (Grant No. 203/05/H001), and the Ministry of Education (Grant No. LC512); it was also a part of the research project Z4 055 0506.

[1] D. Mathur, Phys. Rep. **391**, 1 (2004).
[2] D. Schröder and H. Schwarz, J. Phys. Chem. A **103**, 7385 (1999).
[3] S. D. Price, J. Chem. Soc., Faraday Trans. **93**, 2451 (1997).
[4] S. G. Cox, A. D. J. Critchley, P. S. Kreynin, I. R. McNab, R. C. Shiell, and F. E. Smith, Phys. Chem. Chem. Phys. **5**, 663 (2003).
[5] Z. Herman, Int. Rev. Phys. Chem. **15**, 299 (1996).
[6] A. Hishikawa, H. Hasegawa, and K. Yamanouchi, Chem. Phys. Lett. **361**, 245 (2002).
[7] A. Hishikawa, H. Hasegawa, and K. Yamanouchi, Chem. Phys. Lett. **388**, 1 (2004).
[8] M. Hochlaf, R. I. Hall, F. Penent, J. H. D. Eland, and P. Lablanquie, Chem. Phys. **234**, 249 (1998).
[9] A. Hishikawa, M. Ueyama, and K. Yamanouchi, J. Chem. Phys. **122**, 151104 (2005).
[10] M. Hochlaf, G. Chambaud, and P. Rosmus, J. Chem. Phys. **108**, 4047 (1998).
[11] U. Alkemper and F. von Busch, J. Electron Spectrosc. Relat. Phenom. **93**, 115 (1998).
[12] V. Krishnamurthi, M. Krishnamurthy, V. Marathe, and D. Mathur, J. Phys. B **25**, 5149 (1992).
[13] T. Šedivcová, P. R. Žd'ánská, V. Špirko, and J. Fišer, J. Chem. Phys. **124**, 214303 (2006).
[14] H.-J. Werner and P. Knowles, J. Chem. Phys. **89**, 5803 (1988).
[15] P. Knowles and H.-J. Werner, Chem. Phys. Lett. **145**, 514 (1988).
[16] K. Raghavachari, G. Trucks, J. Pople, and M. Head-Gordon, Chem. Phys. Lett. **157**, 479 (1989).
[17] P. Knowles, C. Hampel, and H.-J. Werner, J. Chem. Phys. **99**, 5219 (1993).
[18] R. J. Gdanitz and R. Ahlrichs, Chem. Phys. Lett. **143**, 413 (1988).
[19] T. H. Dunning, Jr., J. Chem. Phys. **90**, 1007 (1989).
[20] D. E. Woon and T. H. Dunning, Jr., J. Chem. Phys. **98**, 1358 (1993).
[21] H.-J. Werner, P. J. Knowles, R. Lindh *et al.*, MOLPRO, version 2002.10, a package of *ab initio* programs, 2005, see http://www.molpro.net
[22] J. Cooley, Math. Comput. **15**, 363 (1961).
[23] E. Y. Sidky and I. Ben-Itzhak, Phys. Rev. A **60**, 3586 (1999).
[24] V. A. Mandelshtam, T. R. Ravuri, and H. S. Taylor, Phys. Rev. Lett. **70**, 1932 (1993).
[25] V. A. Mandelshtam, H. S. Taylor, V. Ryaboy, and N. Moiseyev, Phys. Rev. A **50**, 2764 (1994).
[26] V. Špirko, M. Rozložník, and J. Čížek, Phys. Rev. A **61**, 014102 (2000).
[27] K. Huber and G. Herzberg, *Molecular Spectra and Molecular Structure IV: Constants of Diatomic Molecules* (Van Nostrand, New York, 1979).
[28] Y. Liu, C. Duan, J. Liu, L. Wu, C. Xu, Y. Chen, P. Hamilton, and P. B. Davies, J. Chem. Phys. **116**, 9768 (2002).
[29] M. Hochlaf, G. Chambaud, P. Rosmus, T. Andersen, and H. Werner, J. Chem. Phys. **110**, 11835 (1999).
[30] C. Destandau, G. Chambaud, and P. Rosmus, J. Chem. Phys. **94**, 1794 (1997).
[31] J. H. D. Eland, M. Hochlaf, G. C. King, P. S. Kreynin, R. J. LeRoy, I. R. McNab, and J.-M. Robbe, J. Phys. B **37**, 3197 (2004).
[32] C. E. Moore, *Atomic Energy Levels*, Natl. Bur. Stand. (U.S.) Circ. No. 467 (U.S. GPO, Washington, DC, 1949).
[33] J. Dyke, S. Gamblin, D. Haggerston, A. Morris, S. Stranges, J. West, T. Wright, and A. Wright, J. Chem. Phys. **108**, 6258 (1998).
[34] P. Coppens and J. Drowart, Chem. Phys. Lett. **243**, 108 (1995).
[35] L. H. Andersen, J. H. Posthumus, O. Vahtras, H. Ågren, N. Elander, A. Nunez, A. Scrinzi, M. Natiello, and M. Larsson, Phys. Rev. Lett. **71**, 1812 (1993).
[36] B. R. Johnson, J. Chem. Phys. **69**, 4678 (1978).

Downloaded 26 Oct 2006 to 130.183.82.42. Redistribution subject to AIP license or copyright, see http://jcp.aip.org/jcp/copyright.jsp

Radiative transition probabilities of CO^{2+}

Tereza Šedivcová, Petra Žďánská-Kaprálová
and Vladimír Špirko[1]

Center for Biomolecules and Complex Molecular Systems, Institute of Organic Chemistry and Biochemistry, Academy of Sciences of the Czech Republic, Flemingovo nám. 2, CZ-166 10 Praha 6, Czech Republic

Abstract

Radiative transition probabilities (Einstein A coefficients), Franck-Condon factors and radiative lifetimes are determined for the $X^3\Pi$, $^3\Sigma^-$, $a^1\Sigma^+$, $^1\Pi$, $c^1\Delta$ and $A^3\Sigma^+$ states of the CO^{2+} dication using *ab initio* potential energy, spin-orbit coupling, electric dipole and electronic transition moment functions and the standard complex-scaling method. The calculated radiative lifetimes of the upper electronic states of the spin-allowed $A^3\Sigma^+$ $X^3\Pi$ and $b^1\Pi$ $a^1\Sigma^+$ transitions are longer than their predissociating lifetimes, explaining thus the attempts made so far to observe CO^{2+} in the optical spectral region.

1 Introduction

Only two rotationally resolved optical spectra of doubly charged molecular ions have been reported in the literature so far, namely the optical emission spectra of NO^{2+} and N_2^{2+} (see Refs. [1–4,?]). Rather surprisingly, despite a strong experimental and theoretical effort, no photon emission has definitely been detected from CO^{2+}. There are three principal reasons which may account for this failure [2]: (1) The electronic states involved in the allowed transitions are strongly predissociated by a tunnel effect through their potential barriers or by spin-orbit interaction with repulsive states. (2) The lower states have lifetimes too short to allow the CO^{2+} ion to reach the detector. (3) The total emission intensity of the spectrum does not attain the threshold of photon detection.
Based on the available experimental [5–7] and theoretical [8] data, the electronic ground states of the discussed transitions are characterised by vibra-

[1] Corresponding author. E-mail: spirko@marge.uochb.cas.cz

tional states with lifetimes long enough to allow for the safe elimination of reason (2) from the list of important detection drawbacks. Similarly, relying on close similarity of the electronic $\Sigma^+ - \Pi$ transition moments of CO^{2+} and CO^+ and successful spectral observations of the latter cation, it may be surmised [2] that reason (3) cannot cause real difficulties for observing the CO^{2+} emission spectrum, for instance by means of the translational energy loss spectroscopy [9] or photoion-fluorescence photon coincidence experiments [10]. Consequently, reason (1) seems to be the only principal limitation for observing the CO^{2+} emission spectra in the optical region.
Strictly speaking, the formulation of reason (1) above is not quite relevant. To make it more complete, the predissociation decays of the discussed states should be related to their radiative counterparts. To allow for it, we have decided to evaluate these characteristics theoretically, using high level *ab initio* calculations.

2 The coupled Hamiltonian

In order to solve the fully coupled problem including electronic and nuclear degrees of freedom of the diatomic systems, we assume that the total wavefunction is obtained in the Born-Oppenheimer approximation based on rotationally adiabatic electronic potentials, $U^{\rm eff}_{nJp}(R)$ [11,12]. The adiabatic potentials $U^{\rm eff}_{nJp}(R)$ are defined as solutions of the effective rotational-electronic Hamiltonian $\hat{H}_{\rm eff}$ and associated with well defined electronic quantum numbers (n), angular quantum numbers (J), and the parity (p). $\hat{H}_{\rm eff}$ is given by

$$\hat{H}_{\rm eff} = \hat{H}_{\rm el} + \hat{H}_{\rm so} + \hat{H}_{\rm rot}, \tag{1}$$

where $\hat{H}_{\rm el}$ is the spin-free electronic Hamiltonian, $\hat{H}_{\rm so}$ is the spin-orbit coupling operator, and $\hat{H}_{\rm rot}$ is the nuclear rotational Hamiltonian defined as

$$\hat{H}_{\rm rot} = B\,||\,\hat{\mathbf{J}} - \hat{\mathbf{L}} - \hat{\mathbf{S}}\,||^2, \tag{2}$$

with $\hat{\mathbf{J}}$, $\hat{\mathbf{L}}$ and $\hat{\mathbf{S}}$ being the total, electronic orbital and spin angular momentum operators, respectively, and $B = 1/(2\mu R^2)$ being the rotational constant for the diatomic.

The Hamiltonian $\hat{H}_{\rm eff}$ is expanded in the basis set given by parity-defined rotational-electronic eigenfunctions $|n, \Lambda, S, J, \Omega, p\rangle$ of Hund's case (a) [11,12], where the quantum numbers have their conventional meaning, i.e. Ω and Λ are projections of the J and L onto the internuclear axis. The Hamiltonian is partitioned into matrices $\mathbf{H}_{J,p}$ for every rotational number J and parity p. Accordingly, each of the $\mathbf{H}_{J,p}$ matrices connects different electronic and

rotational quantum numbers n, Λ, S, and Ω. Ω is restricted by the electronic quantum numbers $\Omega = \Lambda + \Sigma$, where Σ is a projection of S onto the internuclear axis. In the case of the CO^{2+} dication, we consider the six lowest electronic states, $A^3\Sigma^+$, $c^1\Delta$, $b^1\Pi$, $a^1\Sigma^+$, $^3\Sigma^-$, and $X^3\Pi$. Thus the Hamiltonian matrices $\mathbf{H}_{J,p=e}$ for the even parity are constructed in the basis set of the e states given by $A^3\Sigma_1^+$, $c^1\Delta_2$, $b^1\Pi_1$, $a^1\Sigma_0^+$, $^3\Sigma_0^-$, $^3\Sigma_1^-$, $X^3\Pi_0$, $X^3\Pi_1$ and $X^3\Pi_2$. The Hamiltonian matrices $\mathbf{H}_{J,p=f}$ for the odd parity are constructed using the f states given by $A^3\Sigma_0^+$, $A^3\Sigma_1^+$, $c^1\Delta_2$, $b^1\Pi_1$, $^3\Sigma_1^-$, $X^3\Pi_0$, $X^3\Pi_1$ and $X^3\Pi_2$. (The subscript denotes Ω. Some terms are obviously not included for $J < 2$ due to the requirement $\Omega \leq J$.) The lower triangle parts of the Hamiltonian matrices $\mathbf{H}_{J,p}$ are given in Tables 1 and 2. (Note the selection rule $\Delta\Omega = \Delta\Lambda$ for the matrix elements arising from the fact that only terms with same spin projections Σ are coupled by $\hat{H}_{\rm rot}$ [13].)

The Hamiltonian matrices $\hat{\mathbf{H}}_{\rm eff}$, which are parametrically R dependent, define the rotationally adiabatic rovibronic Hamiltonian in the basis set given by parity-defined rotational-electronic eigenfunctions of such a Hund's case (a) that

$$\hat{\mathbf{H}}_{\rm eff}(R) = -\frac{\hbar^2}{2\mu}\frac{d^2}{dR^2}\mathbf{I} + \mathbf{H}_{J,p}(R), \tag{3}$$

where $\mathbf{I}$ is the unity matrix. $\mathbf{H}_{J,p}(R)$ is further expanded in the finite-box basis set and diagonalised by standard diagonalisation programs.

3 Computational details

The vibrational and electronic transition dipole moment functions are calculated using the same internally contracted multireference configuration interaction (icMRCI) procedure [14,15] as in the case of our previous calculation of the potential energy and spin-orbit coupling functions [8].

Resonances are calculated using the standard complex-scaling (c-s) approach [16]. The physical Hamiltonian $\hat{\mathbf{H}}_{\rm eff}(R)$ is transformed using the complex rotation of the coordinate $R \rightarrow Re^{i\theta}$, where θ is a complex-scaling parameter $0 \leq \theta < \pi/4$. Resonances are obtained as square integrable solutions of the transformed Hamiltonian given by,

$$\hat{\mathbf{H}}_{\rm eff}^{\theta} = -\frac{\hbar^2 e^{-2i\theta}}{2\mu}\frac{d^2}{dR^2}\mathbf{I} + \hat{\mathbf{H}}_{J,p}(Re^{i\theta}), \tag{4}$$

for $\theta > \theta_{crit}$. The complex eigenvalues of resonances are stable with respect to varied the parameter θ, which makes it possible to recognise them among

Table 1. Matrix elements of $H_{J,p}$ in the Hund's case (a) basis set for e parity. $U(^3\Sigma^+)$, $U(^1\Pi)$, etc. are BO potentials. H_{SO1-10} mark the *s-o* couplings. A is the spin-orbit constant of the $X^3\Pi$ state (taken from Table 1 of Ref. [2]). $z = J(J+1)$ and $B = 1/2\mu R^2$.

	$\vert^3\Sigma_1^+\rangle$	$\vert^1\Delta_2\rangle$	$\vert^1\Pi_1\rangle$	$\vert^3\Sigma_1^-\rangle$	$\vert^3\Sigma_0^-\rangle$	$\vert^3\Pi_2\rangle$	$\vert^3\Pi_1\rangle$	$\vert^3\Pi_0\rangle$	$\vert^1\Sigma_0^+\rangle$
$\langle^3\Sigma_1^+\vert$	$U(^3\Sigma^+)+Bz$								
$\langle^1\Delta_2\vert$	0	$U(^1\Delta)+B(z+6)$							
$\langle^1\Pi_1\vert$	H_{SO1}	$-B2\sqrt{z-2}$	$U(^1\Pi)+Bz$						
$\langle^3\Sigma_1^-\vert$	H_{SO2}	0	H_{SO3}	$U(^3\Sigma^-)+Bz$					
$\langle^3\Sigma_0^-\vert$	$H_{SO2}-B\sqrt{2z}$	0	H_{SO3}	$-B\sqrt{2z}$	$U(^3\Sigma^-)+B(z+2)$				
$\langle^3\Pi_2\vert$	$H_{SO4}-B\sqrt{2(z-2)}$	H_{SO5}	H_{SO6}	$H_{SO6}-B\sqrt{2(z-2)}$	H_{SO7}	$U(^3\Pi)+A+B(z-2)$			
$\langle^3\Pi_1\vert$	$H_{SO4}+2B$	H_{SO5}	H_{SO6}	$H_{SO6}+2B$	$H_{SO7}-B\sqrt{2z}$	$-B\sqrt{2(z-2)}$	$U(^3\Pi)+B(z+2)$		
$\langle^3\Pi_0\vert$	$H_{SO4}+B\sqrt{2z}$	H_{SO5}	H_{SO6}	$H_{SO6}+B\sqrt{2z}$	$H_{SO7}+2B$	0	$-B\sqrt{2z}$	$U(^3\Pi)-A+B(z+4)$	
$\langle^1\Sigma_0^+\vert$	H_{SO8}	0	$-B\sqrt{2z}$	H_{SO9}	H_{SO9}	H_{SO10}	H_{SO10}	H_{SO10}	$U(^1\Sigma^+)+Bz$

Table 2. Matrix elements of $H_{J,p}$ in the Hund's case (a) basis set for f parity. $U(^3\Sigma^+)$, $U(^1\Pi)$, etc. are BO potentials, H_{SO1-7} mark the s-o couplings, A is the spin-orbit constant of the $X^3\Pi$ state (taken from Table 1 of Ref. [2]), $z = J(J+1)$ and $B = 1/2\mu R^2$.

	$\vert^3\Sigma_1^+\rangle$	$\vert^1\Delta_2\rangle$	$\vert^1\Pi_1\rangle$	$\vert^3\Sigma_1^-\rangle$	$\vert^3\Pi_2\rangle$	$\vert^3\Pi_1\rangle$	$\vert^3\Pi_0\rangle$	$\vert^3\Sigma_0^+\rangle$
$\langle^3\Sigma_1^+\vert$	$U(^3\Sigma^+)+Bz$							
$\langle^1\Delta_2\vert$	0	$U(^1\Delta)+B(z+6)$						
$\langle^1\Pi_1\vert$	H_{SO1}	$-B2\sqrt{z-2}$	$U(^1\Pi)+Bz$					
$\langle^3\Sigma_1^-\vert$	H_{SO2}	0	H_{SO3}	$U(^3\Sigma^-)+Bz$				
$\langle^3\Pi_2\vert$	$H_{SO4}-B\sqrt{2(z-2)}$	H_{SO5}	H_{SO6}	$H_{SO7}-B\sqrt{2(z-2)}$	$U(^3\Pi)+A+B(z-2)$			
$\langle^3\Pi_1\vert$	$H_{SO4}+2B$	H_{SO5}	H_{SO6}	$H_{SO7}+2B$	$-B\sqrt{2(z-2)}$	$U(^3\Pi)+B(z+2)$		
$\langle^3\Pi_0\vert$	$H_{SO4}-B\sqrt{2z}$	H_{SO5}	H_{SO6}	$H_{SO7}-B\sqrt{2z}$	0	$-B\sqrt{2z}$	$U(^3\Pi)-A+B(z+4)$	
$\langle^3\Sigma_0^+\vert$	$-B\sqrt{2z}$	0	H_{SO1}	$H_{SO2}-B\sqrt{2z}$	H_{SO4}	$H_{SO4}-B\sqrt{2z}$	$H_{SO4}+2B$	$U(^3\Sigma^+)+B(z+2)$

other complex solutions. The complex resonance eigenvalues, being defined as $\epsilon_r - i\Gamma_r/2$, provide the resonance positions ϵ_r and widths Γ_r.

Construction of the complex-scaled Hamiltonian requires complex rotation of the functions $U(R)$ and $H_{SO1-10}(R)$. This is done by fitting to analytical functions used in our previous work [8].

4 Integral resonance-to-resonance emission probability

In this section, we focus on defining probability for spontaneous emission from rovibronic states on excited electronic surfaces to rovibronic states on the ground electronic surface. State-to-state transition probability $A(i \to f)$ is defined by the following expression

$$A(i \to f) = K\,\omega^3_{i\to f}\,|\langle v_i|\mu_{T_M}(R)|v_f\rangle|^2, \tag{5}$$

where $\mu_{0T_M}(R)$ is the *ab initio* electronic transition moment (calculated here using the `MOLPRO` suite [17]); ω is given by the transition frequency defined as $\hbar\omega = E_i - E_f$; and the multiplication constant $K = 7.2356 \times 10^{-6}$ is the appropriate factor to express the probability in s^{-1} when the transition moment is given in units of eÅ and the energy in cm^{-1}. In the case of the CO^{2+} dication, v_i and v_f stand for continuum rovibronic states as the diatomic is allowed to dissociate on all potential surfaces. Thus $A(i \to f) \equiv A(E_i \to E_f)$ defines the continuum-to-continuum emission probabilities for the transition between the rovibronic energies E_i and E_f.

In the case of narrow non-overlapping resonances, it is reasonable to assume that the system is preferentially prepared in the close resonance energies where the density of continuum states is very high. Similarly, we may assume that the spontaneous emission preferentially leads to predissociation states of the ground electronic surface in close proximity of resonances. Therefore, in the case of narrow resonances, it is sensible to define the integral resonance-to-resonance emission probability, such that

$$A_{\rm int}(r_i \to r_f) = \int_{\epsilon_{ri}-a\Gamma_{ri}}^{\epsilon_{ri}+a\Gamma_{ri}} dE_i \int_{\epsilon_{rf}-a\Gamma_{rf}}^{\epsilon_{rf}+a\Gamma_{rf}} dE_f\; A(E_i \to E_f), \tag{6}$$

where we integrate the continuum-to-continuum emission probabilities in the vicinity of the two participating resonances. ϵ_{ri} and ϵ_{rf} represent the positions of the two participating resonances, whereas Γ_{ri} and Γ_{rf} denote their widths. The factor $a \gg 1$ is adjusted in such a way that only single resonances i and f contribute to $A_{\rm int}(r_i \to r_f)$.

The integral emission probabilities $A_{\rm int}(r_i \to r_f)$ are to be evaluated based on complex-scaled non-hermitian resonance wavefunctions. To the best of our knowledge, continuum-to-continuum transition probabilities are not suitably defined using the complex-scaled wavefunctions. However, the exact formula for continuum-to-bound state transition probabilities is available, derived e.g. by Andric et al. [18]:

$$A(i \to f) = K\,\omega_{i\to f}^3 \sum_{ri=1}^{N} \frac{\mathrm{Im}\, C_{ri,f}(E_i - \epsilon_{ri}) - \mathrm{Re}\, C_{ri,f}\Gamma_{ri}/2}{(E_i - \epsilon_{ri})^2 + \Gamma_{ri}^2/4}. \tag{7}$$

where the sum is over resonances and discretised states of rotated continuum on the excited electronic surface. $C_{ri,f}$ is given by

$$C_{ri,f} = (\psi_{ri}^{(l)}|\mu_{T_M}(Re^{i\theta})|\psi_f^{(r)})(\psi_f^{(l)}|\mu_{T_M}(Re^{i\theta})|\psi_{ri}^{(r)}). \tag{8}$$

where ψ_{ri} and ψ_f represent the complex-scaled resonance (initial) and bound (final) states given by solution of $\hat{\mathbf{H}}_{J,p}^{\theta}$. The indices (l) and (r) denote the left and right solutions of the non-hermitian complex-scaled Hamiltonian, respectively, as defined in Ref. [16]. (The left vector is defined as solution of the transposed complex-scaled Hamiltonian. The wavefunctions are normalised such that $(\psi^{(l)}|\psi^{(r)}) = 1$.) A special bracket notation has been used, where the "bra" wavefunction is not a complex conjugate as usual.

We are about to calculate emission probabilities to the lowest resonance on the ground state electronic surface, which is extremely narrow, hence we completely neglect its finite width and use Eq. 7 as a substitution for the continuum-to-continuum Einstein coefficients in the definition of the integral emission probability, Eq. 6. Neglecting the energy dependence of the prefactor $\omega_{i\to f}^3$, we obtain:

$$A_{\rm int}(r_i \to r_f) \approx K\,\omega_{ri\to rf}^3\,(\psi_{ri}^{(l)}|\mu_{T_M}(Re^{i\theta})|\psi_{rf}^{(r)})(\psi_{rf}^{(l)}|\mu_{T_M}(Re^{i\theta})|\psi_{ri}^{(r)}). \tag{9}$$

where ψ_{rf} is the final resonance wavefunction whose position is given by ϵ_{rf} and $\hbar\omega_{ri\to rf} = \epsilon_{ri} - \epsilon_{rf}$.

The integral Einstein coefficients make it possible to calculate the radiative lifetimes associated with individual resonances on excited electronic states, such that $\tau_{ri} = 1/A_{\rm int}(r_i \to r_f)$ [19].

4.1 Absolute intensity

Absolute intensities of possible rovibronic emission transitions from $A^3\Sigma^+$, $v' = 0$, $J' = 1$ have been calculated using the well-known formula [13]

$$I_{em}^{v'v''} = \frac{64}{3}\pi^4 c S_J N_{J'v'} \nu^4 t^2, \tag{10}$$

where $t = (v_{ri}^{(l)}|\mu_{TM}(Re^{i\theta})|v_{rf}^{(r)})(v_{rf}^{(l)}|\mu_{TM}(Re^{i\theta})|v_{ri}^{(r)})$, μ being the appropriate complex-scaled transition matrix element, ν being frequency of transition and c being the speed of light. $N_{J'v'}$ is the number of molecules in the rovibronic state v_{ri} determined using the Boltzmann distribution law

$$N_{J'v'} = \frac{N}{q^r q^v}(2J+1)e^{-E_{J'v'}/kT}, \tag{11}$$

with N as the total number of molecules CO^{2+} in the sample, q^r and q^v rotational and vibrational partition functions, k and T Boltzmann constants and the temperature, respectively. S_J are Hönl-London factors ($(2J+1)/4$, $(J-1)/4$ and $(J+2)/4$ for the Q, R and P branch in our case, respectively). Intensities were calculated for the number of molecules of CO^{2+} in 1 l under standard conditions.

5 Results and discussion

The potential energy functions and vibrational and electronic electric dipole moment functions calculated for the $X^3\Pi$, $^3\Sigma^-$, $a^1\Sigma^+$, $b^1\Pi$, $c^1\Delta$ and $A^3\Sigma^+$ states and $X^3\Pi \rightarrow {}^3\Sigma^-$, $X^3\Pi \rightarrow A^3\Sigma^+$, $a^1\Sigma^+ \rightarrow b^1\Pi$ and $b^1\Pi \rightarrow c^1\Delta$ transitions are shown in Figs. 1-3. The corresponding Einstein coefficients of spontaneous emission ($A_{v'v''}$), transition dipole matrix elements ($T_{v'v''}$) and band origin wavelengths of the vibronic spin-forbidden transitions $a^1\Sigma^+ \rightarrow X^3\Pi$ and $b^1\Pi \rightarrow X^3\Pi$ and spin-allowed transitions $A^3\Sigma^+ \rightarrow X^3\Pi$ and $b^1\Pi \rightarrow a^1\Sigma^+$ are collected in Tables 3-6.

Tables 3 and 4 show values for the spin-forbidden transitions (arising through the mixing of wavefunctions caused by the *s-o* interaction), which are only three times smaller than values for the spin-allowed transitions. Both the numerically exact ("6-state") and approximate (Franck-Condon and "2-state") values of the calculated characteristics are of the same order of magnitude, thus it can be concluded that the latter approximations are fairly reasonable. Apparently, the values depend mainly on the *s-o* interaction between the electronic states which are involved directly in the corresponding transitions; the

remaining states cause only smaller perturbations. In this regard, a very similar situation also occurs in the case of the spin-allowed transitions, for which, however, we observe fairly profound breakdown of the FC approximation (see Tables 5 and 6). The vibronic energies and predissociation and radiative lifetimes of the studied vibronic states are available either in Table 7 or by simply combining these data with the data given in Tables 3-6. As can be seen in Table 7, the calculated energies agree well with the measured values (based on our calculations, the v=0 vibrational state of the $A^3\Sigma^+$ data of Ref. [20] belongs to another electronic state, and the vibrational labels v of the remaining states should be replaced by $v-1$).

Relying on the agreement between the calculated and experimental vibronic energies, we consider it legitimate to assume that the calculated radiative characteristics are obtained with reliable accuracy. Therefore, when these data are used, the molecular rovibrational spectrum of CO^{2+} can be predicted accurately for all its experimentally studied states and thus help in their detecting and rationalising. Until now, despite rather favourable transition moments, only few rovibronic spectral lines have been found which seem to belong to the CO^{2+} cation, namely six emissions which have been attributed to the $P_{33}(1)$ and $P_{23}(1)$ lines in the (0,0),(0,1) and (0,2) subbands of the $A^3\Sigma^+$ $X^3\Pi$ transition [2]. A plausible explanation of the scarcity of the emission lines can be deduced from a brief inspection of Table 7. In the table we can see that the radiative lifetimes are by orders of magnitude longer than their predissociation analogues, thus proving the very low probability of the radiative transfers and predominance of the dissociation decays. Consequently, based on the theory, no emission can be expected from the studied states. Strictly speaking, however, the calculated predissociation lifetimes are physically correct only for the J=0 states. Accordingly, prior to making final conclusions, we found it necessary to investigate the role of the centrifugal distortion barriers confining the J>0 states. As a matter of fact, considering the relatively very small centrifugal barriers has led to a spectacular increase in the predissociation lifetimes for the J=1 states of the $A^3\Sigma^+_1$ electronic state (see Table 8). The increase appears large enough to allow for observable emission from these states (only these states!) and, consequently, to arrive finally at a gratifying agreement with the experiment, as can be seen in Table 9.

6 Conclusions

The potential energy curves, spin-orbit coupling and electric dipole transition moments of the six lowest electronic states of CO^{2+} were used to calculate the transition moment matrix elements and Franck-Condon factors for the spin-forbidden $a^1\Sigma^+ \rightarrow X^3\Pi$ and $b^1\Pi \rightarrow X^3\Pi$ and spin-allowed $A^3\Sigma^+ \rightarrow X^3\Pi$ and $b^1\Pi \rightarrow a^1\Sigma^+$ transitions using the complex-scaling method. The

calculated characteristics depend predominantly only on the *s-o* interaction between the states involved directly in the transitions, with the remaining states causing only small perturbations. The Franck-Condon approximation works satisfactorily only in the case of the spin-forbidden transitions which appear only about 3 orders of magnitude weaker than the allowed transitions.

With a strict exception for the J=1 rotational states of the $A^3\Sigma_1^+$ electronic state, the calculated radiative lifetimes are too long to allow for observable emissions. This fact, found in full accord with the experiment, implies strong limits for detecting rotationally resolved optical spectra of CO^{2+}. Moreover, it proves fairly dim prospects for the formation of the long-living meta-stable states of the ground electronic state of CO^{2+} via radiative processes.

Acknowledgements

The authors wish to thank The Supercomputer MetaCenters of Charles University, Prague, and Masaryk University, Brno, for the time devoted to the project. The study was supported by the Ministry of Education (grant No. LC512), the Grant Agency of the Czech Republic (203/05/H001 and 203/06/0420) and the Grant Agency of the Academy of Sciences of the Czech Republic (KJB100550501).

References

[1] J. H. D. Eland, M. Hochlaf, G. C. King, P. S. Kreynin, R. J. LeRoy, I. R. McNab, J. M. Robbe, J. Phys. B: At. Mol. Opt. Phys. 37 (2004) 3197.

[2] D. Cossart, J. M. Robbe, Chem. Phys. Lett. 311 (1999) 248.

[3] D. Cossart, F. Launay, J. M. Robbe, G. Gandara, J. Mol. Spec. 113 (1985) 142.

[4] D. Cossart, C. Cossart-Magos, J. Mol. Spec. 147 (1991) 471.

[5] M. Lundqvist, P. Baltzer, D. Edvardsson, L. Karlsson, B. Wannberg, Phys. Rev. Lett. 75 (1995) 1058.

[6] L. H. Andersen, J. H. Posthumus, O. Vahtras, H. Ågren, N. Elander, A. Nunez, A. Scrinzi, M. Natiello, M. Larsson, Phys. Rev. Lett. 71 (1993) 1812.

[7] F. Penent, R. I. Hall, R. Panajotović, J. H. D. Eland, G. Chaplier, P. Lablanquie, Phys. Rev. Lett. 81 (1998) 3619.

[8] T. Šedivcová, P. R. Ždánská, V. Špirko, J. Fišer, J. Chem. Phys. 124 (2006) 214303.

[9] Z. Herman, P. Jonathan, A. G. Brenton, J. H. Beynon, Chem. Phys. Lett. 141 (1987) 433.

[10] G. Dujardin, L. Hellner, M. Hamdan, A. G. Brenton, B. J. Olsson, M. J. Besnard-Ramage, J. Phys. B 23 (1990) 1165.

[11] A. Carrington, T. P. Softley, Chem. Phys. 106 (1986) 315.

[12] J. T. Hougen, The Calculation of Rotational Energy Levels and Rotational Line Intensities in Diatomic Molecules, US Natl. Bur. Stand. Monogr. 115.

[13] K. Huber, G. Herzberg, Molecular spectra and molecular structure iv. constants of diatomic molecules (Van Nostrand, New York, 1979).

[14] H.-J. Werner, P. J. Knowles, J. Chem. Phys. 89 (1988) 5803.

[15] P. J. Knowles, H.-J. Werner, Chem. Phys. Lett. 145 (1988) 514.

[16] N. Moiseyev, Phys. Rep. 302 (1998) 211.

[17] H.-J. Werner, P. J. Knowles, R. Lindh, M. Schütz, P. Celani, T. Korona, F. R. Manby, G. Rauhut, R. D. Amos, A. Bernhardsson, A. Berning, D. L. Cooper, M. J. O. Deegan, A. J. Dobbyn, F. Eckert, C. Hampel, G. Hetzer, A. W. Lloyd, S. J. McNicholas, W. Meyer, M. E. Mura, A. Nicklass, P. Palmieri, R. Pitzer, U. Schumann, H. Stoll, A. J. Stone, R. Tarroni, T. Thorsteinsson, Molpro, version 2002.6, a package of ab initio programs, see http://www.molpro.net (2003).

[18] L. Andric, I. Baccarelli, T. P. Grozdanov, R. McCarroll, Phys. Lett. A 298 (2002) 41.

[19] W. T. Zemke, W. C. Stwalley, J. Chem. Phys. 120 (2004) 88.

[20] G. Dawber, A. G. McConkey, L. Avaldi, M. A. MacDonald, G. C. King, R. I. Hall, J. Phys. B: At. Mol. Opt. Phys. 27 (1994) 2191.

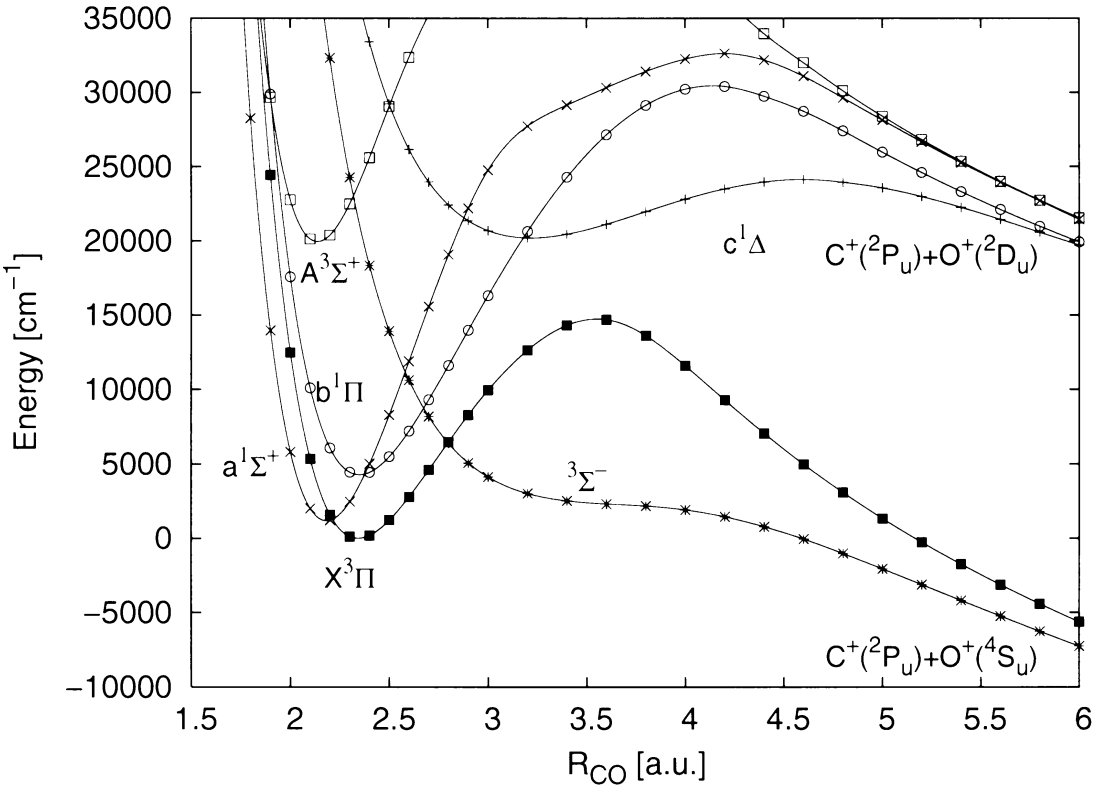

Fig. 1. Potential energy functions of the five lowest electronic states of CO^{2+} in the range of energy $-10\,000$ $30\,000\,\mathrm{cm}^{-1}$.

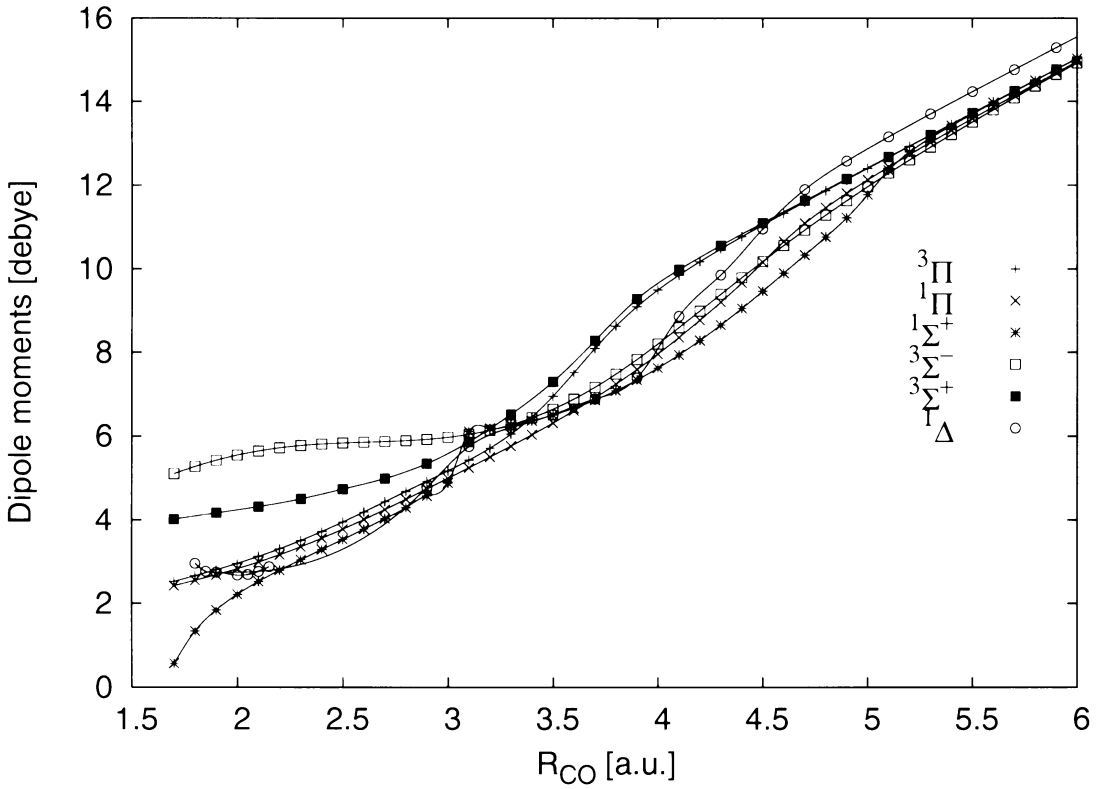

Fig. 2. Calculated electric dipole moment functions for the six lowest states of CO^{2+}.

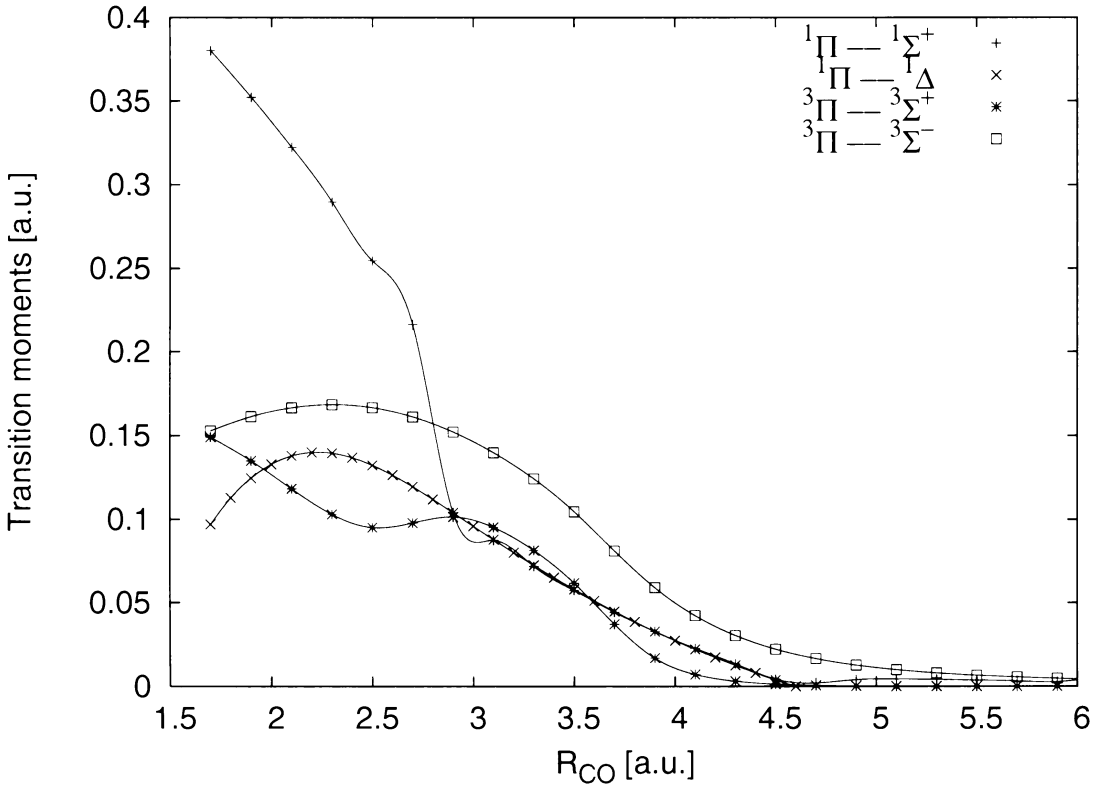

Fig. 3. Calculated electronic transition moment functions for the $^3\Pi$ — $^3\Sigma^-$, $^3\Pi$ — $^3\Sigma^+$, $^1\Sigma^+$ — $^1\Pi$ and $^1\Pi$ — $^1\Delta$ transitions of CO^{2+}.

Table 3
Einstein coefficients, $A_{v'v''}(s^{-1})$, band origin wavelengths, $\nu_{v'v''}$ (cm^{-1}), and transition matrix elements, T (eA), calculated for the $a^1\Sigma^+ \rightarrow X^3\Pi$ transitions.

$v' \backslash v''$		0	1	2	3	4	5
	$A_{v'v''}$	1.525	7.38e−3				
	$\nu_{v'v''}$	1368.9	68.3	1448.1	2783.2	4067.5	5300.2
0	T^a_{exact}	9.07e−3	5.66e−2	1.02e−2	1.54e−3	1.37e−3	0.40e−3
	T^b_{FC}	8.09e−3	5.68e−2	9.59e−3	1.81e−3	1.57e−3	0.86e−3
	T^c_{2st}	1.17e−2	5.36e−2	1.25e−2	0.06e−3	0.28e−3	0.15e−3
	$A_{v'v''}$	2.001	4.893	3.790−3			
	$\nu_{v'v''}$	3312.5	1875.3	495.5	839.6	2123.9	3356.6
1	T^a_{exact}	2.76e−3	1.01e−2	2.06e−3	6.10e−3	3.27e−3	1.10e−3
	T^b_{FC}	4.63e−3	1.24e−3	1.61e−3	2.69e−3	2.69e−3	2.09e−3
	T^c_{2st}	0.43e−3	1.09e−2	3.25e−3	3.98e−3	1.10e−3	0.42e−3
	$A_{v'v''}$	4.987	0.200	0.464	3.42e−3	2.04e−3	
	$\nu_{v'v''}$	5210.0	3772.8	2393.0	1057.9	226.4	1459.1
2	T^a_{exact}	2.21e−3	0.72e−3	2.16e−3	0.63e−3	4.92e−3	0.93e−3
	T^b_{FC}	3.87e−3	2.43e−3	2.98e−3	0.94e−3	1.01e−3	2.14e−3
	T^c_{2st}	0.27e−3	0.89e−3	0.04e−3	0.10e−3	4.12e−3	0.27e−3
	$A_{v'v''}$	4.871	7.319	4.07e−3	0.275	0.94e−3	1.47e−3
	$\nu_{v'v''}$	7064.5	5627.3	4247.5	2912.4	1628.1	395.4
3	T^a_{exact}	1.38e−3	2.38e−3	0.09e−3	1.24e−3	0.17e−3	1.81e−3
	T^b_{FC}	2.58e−3	4.19e−3	$< 10^{-5}$	2.42e−3	2.41e−3	0.70e−3
	T^c_{2st}	0.12e−3	0.19e−3	$< 10^{-5}$	0.46e−3	1.57e−3	2.04e−3
	$A_{v'v''}$	3.147	14.656	6.231	0.973	0.055	0.023
	$\nu_{v'v''}$	8874.1	7436.9	6057.1	4722.0	3437.7	2205.0
4	T^a_{exact}	0.79e−3	2.22e−3	1.97e−3	1.13e−3	0.43e−3	0.55e−3
	T^b_{FC}	1.63e−3	4.32e−3	3.78e−3	1.78e−3	1.30e−3	1.92e−3
	T^c_{2st}	0.04e−3	0.17e−3	0.18e−3	0.12e−3	0.34e−3	1.15e−3
	$A_{v'v''}$	2.142	14.199	20.261	0.085	6.794	4.26e−3
	$\nu_{v'v''}$	10637.6	9200.4	7820.6	6485.5	5201.2	3968.5
5	T^a_{exact}	0.49e−3	1.59e−3	2.42e−3	0.21e−3	2.58e−3	0.10e−3
	T^b_{FC}	1.13e−3	3.37e−3	4.77e−3	0.19e−3	5.08e−3	0.27e−3
	T^c_{2st}	0.01e−3	0.07e−3	0.17e−3	0.07e−3	0.16e−3	0.05e−3

[a]The 6 lowest electronic states involved
[b]Franck-Condon approximation
[c]Only $a^1\Sigma^+$ and $X^3\Pi$ electronic states involved

Table 4
Einstein coefficients, $A_{v'v''}(s^{-1})$, band origin wavelengths, $\nu_{v'v''}$ (cm^{-1}), and transition matrix elements, T $(e\text{Å})$, calculated for the $b^1\Pi \rightarrow X^3\Pi$ transitions.

$v' \setminus v''$		0	1	2	3	4	5
	$A_{v'v''}$	9.396	63.754	0.106	0.02e−3		
	$\nu_{v'v''}$	4298.4	2861.3	1481.4	146.4	1138.0	2370.7
0	T^a_{exact}	4.04e−3	1.94e−2	2.13e−3	0.83e−3	0.65e−3	0.06e−3
	T^b_{FC}	7.15e−3	6.65e−2	7.55e−3	2.97e−3	2.43e−3	0.25e−3
	T^c_{2st}	0.62e−3	0.12e−3	0.02e−3	0.02e−3	0.02e−3	0.002e−3
	$A_{v'v''}$	8.465	299.737	0.244	0.23e−3	0.06e−3	
	$\nu_{v'v''}$	5779.0	4341.9	2962.0	1627.0	342.6	890.1
1	T^a_{exact}	2.46e−3	2.25e−2	1.14e−3	0.09e−3	0.44e−3	0.09e−3
	T^b_{FC}	3.01e−3	7.08e−2	4.47e−3	0.28e−3	1.48e−3	0.27e−3
	T^c_{2st}	0.08e−3	0.65e−3	0.14e−3	0.05e−3	0.03e−3	0.02e−3
	$A_{v'v''}$	7.249	574.85	0.35e−3	0.059	0.023	0.01e−3
	$\nu_{v'v''}$	7226.6	5789.5	4409.6	3074.6	1790.2	557.5
2	T^a_{exact}	1.63e−3	2.02e−2	0.02e−3	0.53e−3	0.74e−3	0.05e−3
	T^b_{FC}	2.15e−3	6.47e−2	3.45e−3	2.79e−3	2.64e−3	0.29e−3
	T^c_{2st}	$< 10^{-5}$	0.13e−3	0.67e−3	0.14e−3	0.08e−3	0.05e−3
	$A_{v'v''}$	3.469	678.13	0.19e−3	0.379	6.61e−2	3.69e−3
	$\nu_{v'v''}$	8641.2	7204.0	5824.1	4489.1	3204.7	1972.0
3	T^a_{exact}	0.86e−3	1.58e−2	0.18e−3	0.76e−3	0.52e−3	0.29e−3
	T^b_{FC}	0.95e−3	4.83e−2	0.34e−3	0.79e−3	1.98e−3	2.46e−3
	T^c_{2st}	0.003e−3	0.006e−3	0.17e−3	0.69e−3	0.12e−3	0.11e−3
	$A_{v'v''}$	3.96e−3	588.56	6.63e−2	0.210	0.681	6.33e−2
	$\nu_{v'v''}$	10038.9	8585.6	7205.7	5870.7	4586.3	3353.6
4	T^a_{exact}	0.02e−3	1.13e−2	0.15e−3	0.38e−3	0.99e−3	0.48e−3
	T^b_{FC}	0.25e−3	3.34e−3	1.45e−3	0.48e−3	1.36e−3	2.05e−3
	T^c_{2st}	$< 10^{-5}$	0.005e−3	0.002e−3	0.22e−3	0.70e−3	0.08e−3
	$A_{v'v''}$	2.183	457.17	0.436	4.209	0.963	0.145
	$\nu_{v'v''}$	11370.8	9933.7	8553.8	7218.8	5934.4	4701.7
5	T^a_{exact}	0.45e−3	8.03e−3	0.31e−3	1.24e−3	0.79e−3	0.44e−3
	T^b_{FC}	0.65e−3	2.388e−2	1.40e−3	3.95e−3	3.19e−3	1.18e−3
	T^c_{2st}	$< 10^{-5}$	$< 10^{-5}$	$< 10^{-5}$	$< 10^{-5}$	0.28e−3	0.70e−3

[a] The 6 lowest electronic states involved
[b] Franck-Condon approximation
[c] Only $a^1\Sigma^+$ and $X^3\Pi$ electronic states involved

Table 5
Einstein coefficients, $A_{v'v''}(s^{-1})$, band origin wavelengths, $\nu_{v'v''}$ (cm^{-1}), and transition matrix elements, T (eA), calculated for the $A^3\Sigma^+ \rightarrow X^3\Pi$ transitions.

$v' \backslash v''$		0	1	2	3	4	5
	$A_{v'v''}$	2.31e+4	3.13e+4	2.77e+4	1.74e+4	9.26e+3	4.43e+3
	$\nu_{v'v''}$	20211.6	18774.5	17394.6	16059.6	14775.2	13542.5
0	T^a_{exact}	1.96e−2	2.55e−2	2.69e−2	2.41e−2	1.99e−2	1.57e−2
	T^b_{FC}	0.183	0.236	0.247	0.219	0.180	0.140
	T^c_{2st}	1.97e−2	2.62e−2	2.69e−2	2.41e−2	1.99e−2	1.57e−2
	T^d_{2st+FC}	0.183	0.244	0.248	0.219	0.181	0.141
	$A_{v'v''}$	7.21e+4	2.88e+4	1.77e+3	2.48e+3	8.38e+3	9.73e+3
	$\nu_{v'v''}$	22256.3	20819.2	19439.3	18104.3	16819.9	15587.2
1	T^a_{exact}	3.01e−2	2.10e−2	5.76e−3	7.59e−2	1.56e−2	1.88e−2
	T^b_{FC}	0.282	0.196	0.054	0.069	0.142	0.171
	T^c_{2st}	3.01e−2	2.17e−2	5.78e−3	7.62e−3	1.56e−2	1.88e−2
	T^d_{2st+FC}	0.282	0.203	5.43e−2	6.94e−2	0.142	0.170
	$A_{v'v''}$	9.97e+4	2.19e+1	2.30e+4	2.08e+4	5.14e+3	0.607
	$\nu_{v'v''}$	24246.4	22809.3	21429.4	20094.4	18810.0	17577.3
2	T^a_{exact}	3.11e−2	0.51e−3	1.79e−2	1.88e−2	1.03e−2	0.12e−3
	T^b_{FC}	0.293	5.30e−3	0.167	0.175	9.65e−2	2.28e−3
	T^c_{2st}	3.11e−2	0.38e−3	1.79e−2	1.88e−2	1.04e−2	0.162e−3
	T^d_{2st+FC}	0.293	4.07e−3	0.167	0.175	9.68e−2	2.47e−3
	$A_{v'v''}$	7.88e+4	4.09e+4	2.86e+4	1.02e+2	1.26e+4	1.43e+4
	$\nu_{v'v''}$	26175.8	24738.7	23358.8	22023.8	20739.4	19506.7
3	T^a_{exact}	2.46e−2	1.93e−2	1.76e−2	1.14e−3	1.39e−2	1.63e−2
	T^b_{FC}	0.233	0.182	0.166	0.011	0.129	0.152
	T^c_{2st}	2.46e−2	2.01e−2	1.76e−2	1.16e−3	1.39e−2	1.63e−2
	T^d_{2st+FC}	0.232	0.189	0.166	1.02e−2	0.130	0.151

[a] The 6 lowest electronic states involved
[b] Franck-Condon approximation
[c] Only $A^3\Sigma^+$ and $X^3\Pi$ electronic states involved
[d] Only $A^3\Sigma^+$ and $X^3\Pi$ electronic states involved under FC approximation

Table 6
Einstein coefficients, $A_{v'v''}(s^{-1})$, band origin wavelengths, $\nu_{v'v''}$ (cm^{-1}), and transition matrix elements, T $(e\text{Å})$, calculated for the $^1\Pi \rightarrow a^1\Sigma^+$ transitions.

$v' \backslash v''$		0	1	2	3	4	5
	$A_{v'v''}$	9.84e+2	5.67e+1				
	$\nu_{v'v''}$	2929.5	985.9	911.6	2766.1	4575.7	6746.0
0	T^a_{exact}	7.35e−2	9.04e−2	7.04e−2	4.07e−2	1.80e−2	0.06e−3
	T^b_{FC}	0.249	0.324	0.269	0.167	8.18e−2	3.11e−2
	T^c_{2st}	7.61e−2	9.05e−2	7.04e−2	4.07e−2	1.81e−2	6.07e−3
	T^d_{2st+FC}	0.259	0.325	0.269	0.168	8.19e−2	3.12e−2
	$A_{v'v''}$	4.598+3	1.196+2	2.229	0.2749		
	$\nu_{v'v''}$	4410.1	2466.5	569.0	1285.5	3095.1	4858.6
1	T^a_{exact}	8.61e−2	3.32e−2	4.09e−2	7.05e−2	5.76e−2	3.16e−2
	T^b_{FC}	0.282	0.112	0.151	0.275	0.243	0.146
	T^c_{2st}	8.89e−2	3.32e−2	4.09e−2	7.05e−2	5.76e−2	3.16e−2
	T^d_{2st+FC}	0.291	0.324	0.151	0.275	0.243	0.147
	$A_{v'v''}$	8.51e+3	3.04e+2	2.28e+2	1.99e−3		
	$\nu_{v'v''}$	5857.7	3914.1	2016.6	162.1	1647.5	3411.0
2	T^a_{exact}	7.65e−2	2.65e−2	6.19e−2	8.03e−3	4.96e−2	6.23e−2
	T^b_{FC}	0.242	8.91e−2	0.215	2.71e−2	0.198	0.268
	T^c_{2st}	7.91e−2	2.65e−2	6.19e−2	8.07e−3	4.97e−2	6.23e−2
	T^d_{2st+FC}	0.250	8.92e−2	0.215	2.71e−2	0.199	0.268
	$A_{v'v''}$	9.81e+3	3.79e+3	1.88e+2	6.65e+1	0.136	
	$\nu_{v'v''}$	7272.2	5328.6	3431.1	1576.6	233.0	1996.5
3	T^a_{exact}	5.94e−2	5.88e−2	2.53e−2	4.84e−2	3.86e−2	2.24e−2
	T^b_{FC}	0.183	0.189	8.29e−2	0.172	0.142	9.37e−2
	T^c_{2st}	6.14e−2	5.88e−2	2.53e−2	4.85e−2	3.84e−2	2.24e−2
	T^d_{2st+FC}	0.189	0.189	8.29e−2	0.172	0.142	9.37e−2
	$A_{v'v''}$	8.50e+3	9.67e+3	2.76e+2	4.54e+2	4.157	4.064
	$\nu_{v'v''}$	8653.8	6710.2	4812.7	2958.2	1148.6	614.9
4	T^a_{exact}	4.28e−2	6.65e−2	1.85e−2	4.93e−2	1.947	4.91e−2
	T^b_{FC}	0.128	0.207	6.17e−2	0.166	7.16e−2	0.186
	T^c_{2st}	4.41e−2	6.65e−2	1.85e−2	4.93e−2	1.93e−2	4.92e−2
	T^d_{2st+FC}	0.132	0.207	0.06.17	0.166	0.07.16	0.185
	$A_{v'v''}$	6.07e+3	1.37e+4	3.71e+3	1.82e+2	2.65e+2	0.247
	$\nu_{v'v''}$	10001.9	8058.3	6160.8	4306.3	2496.7	733.2
5	T^a_{exact}	2.89e−2	6.02e−2	4.68e−2	1.78e−2	4.85e−2	9.32e−3
	T^b_{FC}	8.49e−2	0.183	0.149	5.63e−2	0.167	3.09e−2
	T^c_{2st}	3.00e−2	6.02e−2	4.69e−2	1.78e−2	4.85e−2	9.32e−3
	T^d_{2st+FC}	8.82e−2	0.182	0.149	5.63e−2	0.167	3.09e−2

[a] The 6 lowest electronic states involved
[b] Franck-Condon approximation
[c] Only $A^3\Sigma^+$ and $X^3\Pi$ electronic states involved
[d] Only $A^3\Sigma^+$ and $X^3\Pi$ electronic states involved under FC approximation

Table 7
The calculated and experimental energies (cm^{-1}) and predissociation $\tau_{pred.}$ and radiative $\tau_{rad.}$ lifetimes (μs) of the vibronic resonances within the $b^1\Pi$, and $A^3\Sigma^+$ and $c^1\Delta$ electronic states.

State v	E_{cal}	E_{exp} [20]	E_{exp} [5]	$\tau_{pred.}$	$\tau_{rad.}$
$b^1\Pi$					
0	1481.3	1516.3	1500.1	30	960.9
1	2961.9	3048.7	2951.9	0.041	211.8
2	4409.5	4524.7	4387.6	6.4×10^{-4}	110.6
3	5824.0	5952.3	5807.1	8.3×10^{-5}	72.2
4	7205.6	7323.4	7194.4	2.3×10^{-4}	52.5
5	8553.7	8638.1	8509.1	1.4×10^{-4}	40.9
6	9868.6	9896.3	9799.5	2.6×10^{-3}	34.3
7	11150.3	11098.1	11065.9	5.5×10^{-4}	29.6
8	12398.4	12251.5	12251.5	2.0×10^{-4}	26.1
9	13612.9	13348.4	13437.1	2.2×10^{-4}	24.8
10	14793.7	14388.9	14598.6	4.5×10^{-4}	23.6
$A^3\Sigma^+$					
0	17394.5	15703.5[a]	17566.7	7.1×10^{-2}	8.97
1	19439.2	17744.1	19663.7	6.6×10^{-3}	7.35
2	21429.3	19736.3	21526.8	2.8×10^{-3}	6.45
3	23358.7	21680.1		3.2×10^{-3}	5.49
4	25221.3	23583.5		1.5×10^{-3}	ϵ
5	27011.0	25438.6		2.1×10^{-4}	ϵ
6	28721.7	27245.3		1.2×10^{-4}	ϵ
7	30348.0	29011.6		1.1×10^{-4}	ϵ
$c^1\Delta$					
0	16918.0			> 10	6.5×10^6
1	17457.6			100	23.5×10^6
2	17981.2			13.7	32.9×10^6
3	18486.9			4.6	20.2×10^6
4	18971.7			2.7	26.4×10^6
5	19431.5			2.2	14.4×10^6
6	19860.1			0.063	6.6×10^6
7	20200.4			7.03×10^{-5}	3.8×10^6

All energy values are taken relative to $X^3\Pi$, $v = 2$ ($E_{X^3\Pi,v=2}$=3549.5 cm^{-1})

[a] Probably belongs to $v = 11$ of $a^1\Sigma^+$ or $b^1\Pi$ state.

ϵ The values for transition moments did not converg.

Table 8
Rovibronic energies E_{rot} (cm^{-1}) and predissociation lifetimes $\tau_{pred.}$ (μs) of the $A^3\Sigma^+$ and $b^1\Pi$ states.

			$A\ ^3\Sigma^+$			
	$v = 0$		$v = 1$		$v = 2$	
J	E_{rot}	$\tau_{pred.}$	E_{rot}	$\tau_{pred.}$	E_{rot}	$\tau_{pred.}$
0	20943.8	0.089	22988.5	0.005	24978.5	$2.4e^{-3}$
1	20947.6	4.01	22992.3	0.223	24982.2	0.106
2	20955.2	0.40	22999.8	0.022	24989.7	0.011
3	20966.7	0.076	23011.1	0.004	25000.9	$2.1e^{-3}$
4	20981.9	0.031	23026.2	$1.7e^{-3}$	25015.7	$8.4e^{-4}$
5	21001.1	0.016	23045.1	$9.4e^{-4}$	25034.4	$4.6e^{-4}$
6	21023.9	0.010	23067.7	$5.9e^{-4}$	25056.7	$2.8e^{-4}$
7	21050.6	0.007	23094.1	$4.0e^{-4}$	25082.7	$1.9e^{-4}$
8	21081.1	0.005	23124.2	$2.9e^{-4}$	25112.5	$1.4e^{-4}$
9	21115.4	0.004	23158.1	$2.2e^{-4}$	25146.0	$1.1e^{-4}$
10	21153.6	0.003	23195.8	$1.7e^{-4}$	25183.2	$0.9e^{-4}$
			$b\ ^1\Pi$			
	$v = 1$		$v = 2$		$v = 3$	
0	6511.4	0.0392	7959.0	$6.17e^{-4}$	9373.5	$8.10e^{-5}$
1	6514.5	0.0389	7962.1	$6.13e^{-4}$	9376.5	$8.08e^{-5}$
2	6520.7	0.0386	7968.2	$6.10e^{-4}$	9382.6	$8.05e^{-5}$
3	6530.1	0.0382	7977.4	$6.06e^{-4}$	9391.6	$8.03e^{-5}$
4	6542.5	0.0377	7989.6	$6.01e^{-4}$	9403.7	$8.01e^{-5}$
5	6558.1	0.0372	8005.0	$5.95e^{-4}$	9418.8	$7.98e^{-5}$
6	6576.7	0.0366	8023.4	$5.89e^{-4}$	9436.9	$7.95e^{-5}$
7	6598.5	0.0359	8044.8	$5.82e^{-4}$	9458.0	$7.92e^{-5}$
8	6623.4	0.0351	8069.3	$5.73e^{-4}$	9482.1	$7.88e^{-5}$
9	6651.4	0.0343	8096.9	$5.65e^{-4}$	9509.3	$7.85e^{-5}$
10	6682.5	0.0335	8127.6	$5.56e^{-4}$	9539.4	$7.81e^{-5}$

Table 9. The calculated energies (cm^{-1}) and absolute intensities ($molcm^{-3}s{-}1$) for the possible $A^3\Sigma^+ \rightarrow X^3\Pi$ transitions (Q and P branches for $J' = 1$, $v' = 0$) and a comparison with the available experiment [2] (P branch for $J' = 0$, $v' = 0$).

Branch	Ω	$v'' = 0$				$v'' = 1$				$v'' = 2$			
		E_{Exp}	E_{Cal}	$E_{Exp-Cal}$	Int.	E_{Exp}	E_{Cal}	$E_{Exp-Cal}$	Int.	E_{Exp}	E_{Cal}	$E_{Exp-Cal}$	Int.
P	0	20310.19	20204.7	105.49	11660	18859.39	18768.41	90.98	14795	17556.43	17388.1	168.3	12143
$J' = 0$	1	20368.84	20266.6	102.24	11803	18918.44	18829.41	89.03	14604	17615.63	17449.4	166.2	11973
ΔE		-58.75	-61.9			-59.05	-61.0			-59.20	-61.3		
Q	0		20208.6		51564		18772.2		64585		17391.9		52952
$J' = 1$	1		20270.0		52194		18833.2		65428		17453.4		53704
ΔE			-61.4				-61.0				-61.5		
P	0		20202.0		51500		18765.7		64495		17385.9		52878
$J' = 1$	1		20264.1		52133		18826.2		65331		17447.6		53634
	2		20321.8		50911		18882.1		63730		17505.8		52174
ΔE_{0-1}			-62.1				-60.5				-61.7		
ΔE_{1-2}			-57.7				-55.9				-58.2		

Molecular Physics, Vol. 104, Nos. 13–14, 10–20 July 2006, 1999–2005

Taylor & Francis
Taylor & Francis Group

Potential energy and transition dipole moment functions of C_2^-†

T. ŠEDIVCOVÁ and V. ŠPIRKO*

Department of Molecular Modeling, Center for Biomolecules and Complex Molecular Systems, Institute of Organic Chemistry and Biochemistry, Academy of Sciences of the Czech Republic, Flemingovo nám. 2, 166 10 Prague 6, Czech Republic

(*Received 29 August 2005; in final form 23 January 2006*)

The potential energy curves of C_2^- in its $^2\Sigma_g^+$, $^2\Pi$ and $^2\Sigma_u^+$ states are constructed by morphing the appropriate icMRCI *ab initio* curves within the framework of the *Reduced Potential Curve* (RPC) approach of Jenč and Plíva. The actual morphing is performed by fitting the RPC parameters to available experimental data. The resulting potential energy curves are in close harmony with these data thus allowing for evaluation of highly accurate wavefunctions of the observed rovibronic molecular states and for reliable interpolation of the so-far unobserved states. Using these wavefunctions and theoretically evaluated electronic transition moment functions, the dipole moment matrix elements are calculated for the allowed transitions among the studied vibronic states. The $^2\Sigma_g^+$ potential energy curve is also used for predicting rotational energies of $^{13}C^{12}C^-$. The calculated data are believed to be useful in searching for spectral evidence of C_2^- both in the laboratory and interstellar medium. Several rotational lines of the $v = 0 - 1$ vibronic band of the $B^2\Sigma_u^+ \rightarrow X^2\Sigma_g^+$ transition are shown to be coincident with absorption features in the spectrum of the carbon star HD 56126.

1. Introduction

Apart from around one hundred neutral molecular species, over twenty positive ions have been detected in the interstellar medium. So far, however, no negatively charged molecular ion has been identified extraterrestrially. The detection of negative ions is a difficult task also in the laboratory. To date, only fifteen anions have been identified in the gas phase using high-resolution spectroscopy [1, 2] and only SH^- and SD^- have been observed [3] in the radio-frequency region which is the most suitable spectral range for extraterrestrial identifications. Negative ions are assumed to play an important role in the formation of interstellar molecules [4] and are also considered as important sources of opacities in cool stars [5, 6]. Therefore, the anions are challenging targets for astronomical searches.

One of the most promising candidates for successful astronomic detection is C_2^-. The anion has already been searched for several times in the visible region using the electronic transition $B^2\Sigma_u^+ \rightarrow X^2\Sigma_g^+$ (see [7] and references therein). Another possibility for detection is provided by the $A^2\Pi_u \rightarrow X^2\Sigma_g^+$ lines which are observable in the infrared region of the molecular spectrum [8] and, at least in principle, by the rotational transitions in the ground electronic state of $^{13}C^{12}C^-$.

Apart from a quantitative wavelength coincidence of the laboratory and extraterrestrial spectra, any successful identification of the searched for species also requires convincing agreement of the spectral intensity patterns. Concerning the $B^2\Sigma_u^+ \rightarrow X^2\Sigma_g^+$ and $A^2\Pi_u \rightarrow X^2\Sigma_g^+$ transitions, the appropriate intensities can be estimated theoretically using, e.g. the MCSCF-SCEP transition moment and potential energy functions of Rosmus and Werner [9]. Though physically correct, the theoretical data are quantitatively less accurate. Thus, we have found it worthwhile to evaluate the sought transition moments using 'experimentally' determined potential energy curves.

The absence of a microwave (sub-millimetre) spectrum deprives C_2^- of a low-temperature cooling mechanism and the molecule can be excited by the stellar and interstellar radiation fields to a supra-thermal temperature ($T_{rot} \geq T_{kin}$). $^{13}C^{12}C^-$, on the other hand, has a small dipole moment and may cool. Therefore, the rotational temperature for $^{13}C^{12}C^-$ may be lower than for $^{12}C^{12}C^-$. Thus, by studying these two molecules simultaneously, important information on the interstellar conditions could be extracted. For these reasons we have also found it worthwhile to predict rovibrational energies of the so-far unobserved $^{13}C^{12}C^-$ anion.

*Corresponding author. Email: spirko@uochb.cas.cz

†Dedicated to Professor Andrzej Sadlej on the occasion of his 65th birthday.

Molecular Physics
ISSN 0026-8976 print/ISSN 1362-3028 online © 2006 Taylor & Francis
http://www.tandf.co.uk/journals
DOI: 10.1080/00268970600662689

2. Computational details

The *ab initio* electronic structure calculations were performed with one-state full valence complete-active-space SCF (CASSCF) and internally contracted multireference configuration interaction (icMRCI) [10–12] methods in D_{2h} symmetry. The atomic orbital basis sets were the augmented correlation-consistent basis sets of Dunning [13] denoted by aug-cc-pV6Z and the full active space consisted of all occupied molecular orbitals (MOs) $1\sigma_g 1\sigma_u 2\sigma_g 2\sigma_u 1\pi_u 3\sigma_g$ and valence MOs $1\pi_g 3\sigma_u$. This approach led to a total of 1798, 1730 and 1798 configuration state functions (CSFs) for the $X^2\Sigma_g^+$, the $^2\Pi_u$ and the $^2\Sigma_u^+$ states, respectively. All CSFs from the CASSCF calculations were taken as reference in the MRCI calculation in which all electrons were correlated. The reference configurations that have contributions more than 0.85 are $1\sigma_g^2 1\sigma_u^2 2\sigma_g^2 2\sigma_u^2 1\pi_u^4 3\sigma_g^1$, $1\sigma_g^2 1\sigma_u^2 2\sigma_g^2 2\sigma_u^2 1\pi_u^3 3\sigma_g^2$ and $1\sigma_g^2 1\sigma_u^2 2\sigma_g^2 2\sigma_u^1 1\pi_u^4 3\sigma_g^2$ for $X^2\Sigma_g^+$, $A^2\Pi_u$ and $B^2\Sigma_u^+$, respectively. The electronic transition moments $^2\Sigma_g^+ \rightarrow {}^2\Sigma_u^+$ and $^2\Sigma_g^+ \rightarrow {}^2\Pi_u$ states were evaluated using the icMRCI wave function with the same set of molecular orbitals. The actual calculations were done with the Molpro suite of *ab initio* programs version 2002.6 [14].

The pointwise calculated *ab initio* energies were smoothed using the following potential energy function, $U(r)$:

$$U(r) = \sum_i F_i \left\{ 1 - \exp[a_1(r - r_e) - a_2(r - r_e)^2 - a_4(r - r_e)^4] \right\}^i, \tag{1}$$

where r is the internuclear distance (r_e being its equilibrium value) and a_1, a_2, a_4 and F_i are fitting parameters. The transition moment functions were smoothed using simple polynomial representations.

The reduced potential curve (RPC) scheme was used in its generalized (GRPC) form [15–17]

$$u = \frac{U}{D_e}, \tag{2}$$

$$\rho = \frac{r - (1 - \alpha \exp[-\beta r/\rho_{ij}])\rho_{ij}}{r_e - (1 - \alpha \exp[-\beta r/\rho_{ij}])\rho_{ij}}, \tag{3}$$

$$\rho_{ij} = \frac{r_e - (\kappa D_e/k_e)^{1/2}}{(1 - \alpha \exp[-\beta r/\rho_{ij}])\rho_{ij}}, \tag{4}$$

where ρ, u and U are the reduced internuclear distance, the reduced energy and the genuine potential, respectively; D_e, r_e and k_e are the depth of the minimum of the potential curve, the equilibrium internuclear distance and the harmonic force constant, respectively; κ is the universal 'reduced' force constant; α and β are 'correction' parameters (in the standard RPC formula, $\kappa = 3.96$, $\alpha = 1$ and $\beta = 1$).

The ro-vibrational energies and wavefunctions were found as eigenvalues and eigenfunctions of the radial Hamiltonian

$$H_{rv} = -\frac{\hbar^2}{2\mu}\frac{d^2}{dr^2} + U(r) + \frac{\hbar^2}{2\mu r^2}N(N+1), \tag{5}$$

where $\hbar$ is Planck's constant, μ is the reduced mass and N is the rotational quantum number. The actual calculations were performed using the Numerov–Cooley numerical integration procedure [18].

Intensities of the studied rovibronic transitions were calculated relative to the transition B X 00 00 (Nv $N'v'$) using the well-known formula [19]

$$I = m(2N+1)P_{NvE}\left(\frac{\nu}{\nu_0}\right)\cdot\left(\frac{t}{t_0}\right)^2, \tag{6}$$

where $t = \langle NvE|\mu(r)|N'v'E'\rangle$ (μ being the appropriate transition moment function), P_{NvE} is the number of molecules in the rovibronic state $|NvE\rangle$ determined using the Boltzmann distribution law and m are Hönl–London factors ($m = N + 1$ and $m = N$ for the R and P branches, respectively). ν_0 is the frequency of the ro-vibronic transition between the ground vibrational levels (00–00), ν is the frequency of the rovibronic transition (NvE–$N'v'E'$) and $t_0 = \langle 00|\mu(r)|0'0'\rangle$.

3. Results and discussion

The calculated potential energy and transition moment functions are displayed in figures 1 and 2 (the data are available on the request from T. Šedivcová). The equilibrium spectroscopic constants derived from the calculated PEFs are collected and compared with available experimental [8, 20] and theoretical data [9] in table 1.

Although reasonably coincident with their experimental counterparts, the spectroscopic constants calculated directly from the *ab initio* potentials cannot meet the accuracy which is necessary for spectral identifications and predictions. To overcome this problem, the potentials were morphed (fitted) to available experimental data within the framework of the RPC approach. The morphing was performed in two steps. Firstly, the standard ($\alpha = 1, \beta = 1$) reduced potential curves were constructed using equations (2)–(4) and the *ab initio* potential curves evaluated in this study.

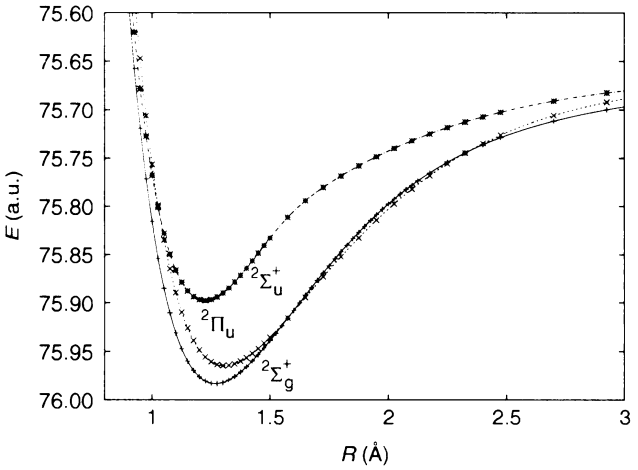

Figure 1. The calculated potential energy functions of the lowest electronic states of the C_2^- anion.

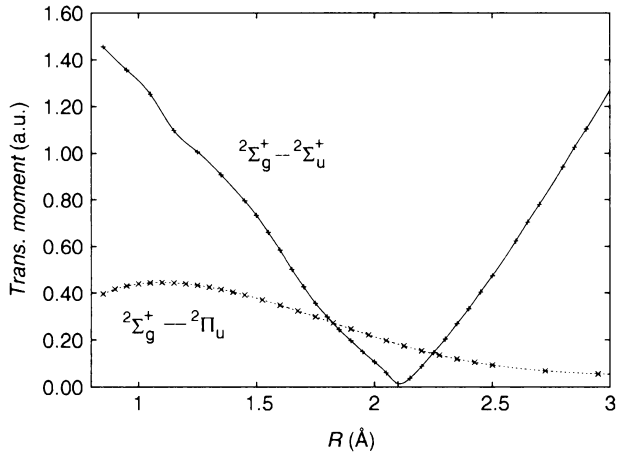

Figure 2. The calculated transition moments of the lowest electronic states of the C_2^- anion.

Table 1. Equilibrium spectroscopic constants of C_2^-.

	$X^2\Sigma_g^+$	$A^2\Pi_u$	$B^2\Sigma_u^+$	Ref.
R_e/Å	1.2685	1.3066	1.2234	
	1.268	1.307	1.223	a
	1.276	1.318	1.231	b
	1.26831(13)	1.30768(13)		c
E_{min}/a.u.	−75.9833	−75.9648	−75.8978	
	−75.8628	−75.8468	−75.7765	a
T_e/cm^{-1}	0.0	4050.6	18763.9	
	0.0	3985.83	18390.8	a
	0.0	3548.8	18594.0	b
	0.0	4064(91)		c
B_e/cm^{-1}	1.7464	1.6458	1.8713	
	1.747	1.643	1.877	a
	1.726	1.619	1.855	b
	1.74666(32)	1.64305(334)		c
w_e/cm^{-1}	1787.40	1679.04	1964.72	
	1781.1	1666.4	1969.1	a
	1780	1646	1983	b
	1781.189(18)	1666.4(10)		c
$w_e x_e$/cm^{-1}	11.56	11.61	10.28	
	11.7	10.8	14.4	a
	12	11.0	16	b
	11.6717(48)	10.80(26)		c
α_e/cm^{-1}	0.0161	0.0159	0.0129	
	0.0167	0.0160	0.0173	a
	0.016	0.016	0.017	b
	0.01651(46)	0.01601(44)		c

[a] From [20].
[b] From [9].
[c] From [8].

Secondly, global potentials were constructed so that their RPCs coicincided with their *ab initio* counterparts and that they provided the best least-squares description of the fitted data [8, 21 23] in terms of the sought parameters D_e, r_e, ρ_{ij}, α and β. The resulting parameters for the lowest electronic states of $^{12}C^{12}C^-$ are presented in table 2. The dereduced potential of the ground electronic state reproduces all available data fairly

quantitatively (see table 3), thus evidencing high reliability of the predicted values for the band centres of the $v=4$ 6 vibrational states, which cannot be derived directly from the available experimental data. Moreover, knowledge of the $v=6$ state allows for accurate prediction of absolute energies of the $v>4$ vibrational states of the $^2\Sigma_u^+$ electronic state which are also inaccessible using the presently available experimental data. Assessing predictive power of the $^2\Pi$ state potential is not as conclusive as in the case of the $^2\Sigma$ states. Nevertheless, a fairly quantitative description of the available data indicates, at least, its adequacy in the equilibrium geometry region.

A very close description of the frequency data of the studied electronic states by means of the morphed *ab initio* potentials supports their adequacy both for accurately predicting the frequency data of the so-far unobserved states and for evaluating the physically correct wavefunctions of the studied ro-vibronic states.

Table 2. GRPC parameters of the electronic states of C_2^-.

Parameters	$X^2\Sigma_g^+$	$A^2\Pi_u$	$B^2\Sigma_u^+$
r_e/Å	1.26825	1.30759	1.22312
ρ_{ij}/Å	0.77635	0.74829	0.84520
D_e/cm^{-1}	61726.7	59500.0[a]	49499.0
α	0.87172	1.0[a]	1.39325
β	0.86[a]	1.0[a]	1.4[a]
St. Dev.	0.026	0.033	0.301

[a]Held fixed after a preliminary determination.

In turn, the wavefunctions can be used for a quantitative evaluation of molecular properties. For instance, the evaluation of the dipole moment matrix elements of the studied electronic states and a correct rationalization of their vibrational dependence (see table 4). Quite generally, knowledge of these matrix elements, defining the intensities of the dipole allowed transitions, is decisively important for any conclusive spectral identification.

The availability of highly reliable intensities for the $B^2\Sigma_u^+ \rightarrow X^2\Sigma_g^+$ rovibronical transition led us to reattempt the search for the C_2^- lines in the stellar spectra recorded recently with the Okayama astrophysical observatory 188 cm telescope (for details see [7]). Unfortunately, the search has not led to any conclusive identification. Nevertheless, as we can see in figure 3 and table 5, for one of the studied carbon stars, namely HD 56126, the search was not completely unsuccessful when assuming C_2^- to be significantly cooler than C_2 which was detected in spectra with a rotational temperature around 240 K [24]. Apart from the spectral peak lying at 4888 Å, all isolated spectral lines pertaining to the *R*-branch of the $v=0-1$ vibronic band of the $X^2\Sigma_g^+ \rightarrow B^2\Sigma_u^+$ transition (i.e. peaks lying at 4870–4895 Å) seem to posses their stellar counterparts. Thus, if we take into account that the 4888 Å absorption may be compensated by the Fe II emission lying at 4887.87 Å [25] and that the *P*-branch lines (i.e. peaks lying at 4898 4902 Å) may be obscured by the coinciding atomic lines, it is plausible that the coinciding absorptions arise due to the C_2^- anion. Unfortunately,

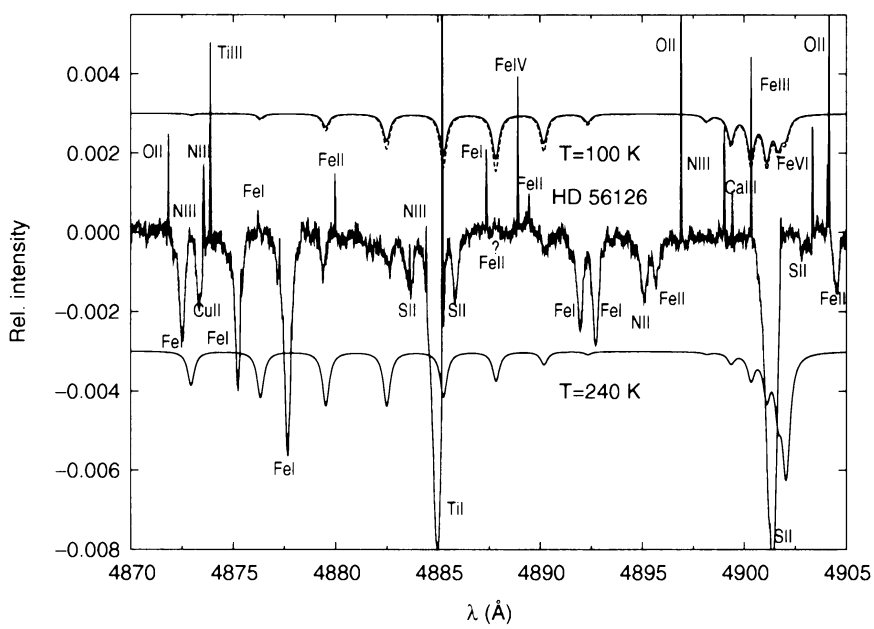

Figure 3. Part of the spectrum for the carbon star HD 56126 and theoretical lines of C_2^- calculated for two different temperatures ($T=100$ and 240 K). The dashed line for $T=100$ K describes results obtained using the Franck–Condon approximation.

Table 3. Vibrational band centres and rotational constants of $^{12}C^{12}C^-$ and $^{13}C^{12}C^-$ (in cm^{-1}).

$^{12}C^{12}C^-$ ground state $X^2\Sigma_g^+$			
v	ν_v	B	$D(10^6)$
0	0	1.73843 [1.73836(19)][a]	6.71094 [6.59(28)][a]
1	1757.8165 [1757.820][c]	1.72171 [1.72186(23)][a]	6.71858 [6.96(38)][a]
2	3492.1939 [3492.204][c]	1.70494 [1.704824(105)][c]	6.72763 [6.65(0.08)][c]
3	5203.1186 [5203.075][c]	1.68813 [1.688057(305)][c]	6.73747 [6.64(0.79)][c]
4	6890.5761	1.67127	6.74809
5	8554.2580	1.6542	6.76339
6	10194.3624	1.63714 [1.637384(608)][c]	6.77826 [6.58(0.45)][c]
7	11810.7364		
8	13403.3121		
9	14972.0194		
10	16516.7859		
Experimental energy above $v=6$			
7	1616.3740 [1616.401][c]	1.62001 [1.620105(599)][c]	6.79473 [6.22(0.44)][c]
8	3208.9897 [3208.931][c]	1.6028 [1.603192(585)][c]	6.81321 [6.51(0.43)][c]
9	4777.6570 [4777.624][c]	1.58551 [1.586235(598)][c]	6.83391 [6.99(0.46)][c]
10	6322.4235 [6322.451][c]	1.56812 [1.567877(933)][c]	6.85595 [5.88(0.82)][c]
Excited state $A^2\Pi_u$			
0	0	1.63511 [1.63501(19)][a]	6.37628 [6.23(29)][a]
1	1644.7899	1.61877 [1.61902(25)][a]	6.39567 [6.72(52)][a]
2	3265.9748	1.60236	6.41446
3	4863.5969	1.58588	6.43287
4	6437.6957	1.56934	6.45159
Excited state $B^2\Sigma_u^+$			
Energy above $X^1\Sigma_g^+ v=0$			
0	18484.034 [18484.034][c]	1.86857 [1.868280(78)][c]	6.85031 [6.84(0.02)][c]
1	20422.734 [20422.827][c]	1.8495 [1.849703(89)][c]	6.91063 [6.89(0.03)][c]
2	22330.079 [22329.783][c]	1.83011 [1.830603(91)][c]	7.0149 [7.02(0.08)][c]
3	24203.728 [24203.140][c]	1.81012 [1.810872(123)][c]	7.16014 [7.30(0.09)][c]
4	26041.211 [26040.19][c]	1.78933 [1.789818(526)][c]	7.34473 [9.55(1.58)][c]
5	27839.949		
6	29597.375		
7	31310.448		
Energy above $X^1\Sigma_g^+ v=6$ $E_v=10194.362$			
5	17645.587 [17645.986][c]	1.76752 [1.768082(633)][c]	7.56932 [7.61(0.49)][c] [7.501(9)][b]
6	19403.013 [19403.645][c]	1.74452 [1.744876(607)][c]	7.83388 [9.01(0.45)][c] [7.790(20)][b]
7	21116.086 [21115.846][c]	1.72017 [1.721075(757)][c]	8.14041 [9.66(0.61)][c] [8.259(29)][b]
$^{13}C^{12}C^-$ ground state $X^1\Sigma_g^+$			
0	0	1.67152	6.20486
1	1724.0218	1.65576	6.21040
2	3425.5093	1.63995	6.21814
3	5104.4494	1.62411	6.22718
4	6760.8287	1.60822	6.23708

[a] From [8].
[b] From [21].
[c] From [22].

Table 4. Transition dipole moment matrix elements calculated using fitted potentials and *ab initio* transition moment functions of C_2^-.

$v \backslash v'$	0	1	2	3	4	5	6	7	8
Transition $X^2\Sigma_g^+ \rightarrow B^2\Sigma_u^+$									
0	0.9216	0.4030	0.1371	0.0402	0.0104	0.0022	0.0003	0.0000	
1	0.3281	0.7659	0.5120	0.2202	0.0764	0.0226	0.0056	0.0010	
2	0.0707	0.4236	0.6276	0.5607	0.2876	0.1143	0.0381	0.0107	0.0023
3	0.0079	0.1133	0.4734	0.5065	0.5758	0.3414	0.1521	0.0562	0.0176
4	0.0002	0.0134	0.1473	0.4989	0.4026	0.5697	0.3824	0.1882	0.0761
5	0.0002	0.0009	0.0173	0.1735	0.5100	0.3160	0.5500	0.4115	0.2210
6	0.0000		0.0026	0.0186	0.1922	0.5127	0.2466	0.5222	0.4301
7			0.0011	0.0054	0.0163	0.2033	0.5111	0.1939	0.4904
8					0.0093	0.0097	0.2066	0.5078	0.1576
9					0.0021	0.0144	0.0019	0.2015	0.5045
Transition $A^2\Pi \rightarrow B^2\Sigma_u^+$									
0	0.5959	0.4328	0.2317	0.1052	0.0425	0.0157	0.0053	0.0016	0.0004
1	0.3855	0.2943	0.4447	0.3253	0.1806	0.0851	0.0356	0.0134	0.0046
2	0.1521	0.4084	0.0729	0.3759	0.3655	0.2422	0.1306	0.0612	0.0256
3	0.0373	0.2169	0.3625	0.0810	0.2773	0.3660	0.2862	0.1746	0.0908
4	0.0036	0.0615	0.2497	0.2908	0.1800	0.1731	0.3381	0.3115	0.2134
5	0.0011	0.0049	0.0786	0.2596	0.2130	0.2360	0.0766	0.2916	0.3188
6	0.0005	0.0033	0.0033	0.0876	0.2534	0.1394	0.2601	0.0051	0.2354
7	0.0001	0.0013	0.0070	0.0018	0.0885	0.2366	0.0754	0.2623	0.0695
8			0.0024	0.0121	0.0111	0.0815	0.2134	0.0226	0.2512
9				0.0034	0.0185	0.0246	0.0672	0.1868	0.0191
Transition $X^2\Sigma_g^+ \rightarrow A^2\Pi$									
0	0.4083	0.1129	0.0171	0.0014	0.0001				
1	0.1248	0.3703	0.1539	0.0292	0.0027	0.0001			
2	0.0312	0.1677	0.3331	0.1812	0.0406	0.0043	0.0002		
3	0.0071	0.0525	0.1946	0.2970	0.2009	0.0516	0.0061	0.0003	
4	0.0015	0.0141	0.0721	0.2122	0.2620	0.2152	0.0622	0.0080	0.0004
5	0.0003	0.0034	0.0220	0.0900	0.2233	0.2281	0.2254	0.0722	0.0100
6		0.0007	0.0059	0.0306	0.1064	0.2293	0.1954	0.2323	0.0818
7		0.0001	0.0014	0.0091	0.0399	0.1213	0.2313	0.1640	0.2364
8			0.0002	0.0023	0.0129	0.0496	0.1345	0.2298	0.1340
9					0.0008	0.0053	0.0223	0.0695	0.1559

Table 5. Coincidences of the C_2 lines for the $X^2\Sigma_g^+ \rightarrow B^2\Sigma_u^+$ band lines found in the stellar spectrum of HD 56126 (in Å).

J	Laboratory peaks $R(J)$	Peaks in stellar spectra	Atomic lines	J	Laboratory peaks $R(J)$	Peaks in stellar spectra	Atomic lines
2	4892.33	4892.34		2	4896.76	4896.90[a]	O II 4896.86
4	4890.18	4890.11		4	4898.16		
6	4887.83	–	Fe II 4887.82	6	4899.35	4899.41[a]	Ca III 4899.31
8	4885.26	4885.25		8	4900.33	4900.34[a]	Fe III 4900.33
10	4882.49	4882.50		10	4901.10	Blended	S II 4901.28
12	4879.52	4879.51		12	4901.66	4901.3 ± 0.40	S II 4901.28
14	4876.39	4876.21[a]	Fe I 4876.18	14	4902.00	Blended	S II 4901.28
16	4872.94	4873.00	N III 4873.10	16	4902.13		
				18	4902.04	Blended	S II 4901.28

[a]Emission peaks.

no similar absorptions were found for the remaining stellar spectra and the discussed identification must be considered as fairly uncertain.

4. Conclusion

The potential energy curves of the $^2\Sigma_g^+$, $^2\Pi$ and $^2\Sigma_u^+$ states of C_2^- were constructed by morphing highly accurate MRCI *ab initio* potentials. The resulting potentials reproduce all of the observed rovibronic data thus allowing for the evaluation of the highly reliable rovibronic wavefunctions of all of the observed molecular states.

Electronic transition moment functions for the dipole allowed transitions among the studied states were evaluated from a highly correlated MRCI wavefunction. Using these functions and the rovibronic wavefunctions pertaining to the morphed potential energy curves, reliable dipole moment matrix elements were evaluated for all studied states. Based on these data, several absorption lines of the $v = 0 - 1$ vibronic band of the $X^2\Sigma_g^+ \rightarrow B^2\Sigma_u^+$ transition were found to be coincident with the absorption peaks in the spectrum of the carbon star HD 56126.

To allow for a spectral detection of C_2^- in the radio frequency region, rotational energies of $^{13}C^{12}C^-$ were predicted accurately using the morphed potential for the $X^2\Sigma_g^+$ state of C_2.

Acknowledgements

This work was supported by the Grant Agency of the Academy of Sciences of the Czech Republic (grant Nos. A400550511 and 203/05/H001) and Ministry of Education (grant No. LC512); it was also a part of the research project 24 055 0506. T. Šedivcová would like to thank computer Metacenter for time allocation.

References

[1] E. Hirota, Chem. Rev. **92,** 141 (1992).
[2] M. Tulej, D. A. Kirkwood, M. Pachkov, and J. P. Maier, Ap. J. **506,** L69 (1998).
[3] S. Civiš, A. Walters, M. Y. Tretyakov, S. Bailleux, and M. Bogey, J. Chem. Phys. **108,** 8369 (1998).
[4] A. Dalgarno and J. H. Black, Rep. Prog. Phys. **39,** 573 (1976).
[5] M. S. Vardya and K. S. Krishna Swamy, Chem. Phys. Lett. **73,** 616 (1980).
[6] D. C. Merlo and L. A. Milone, Astrophys. Space Sci. **288,** 223 (2003).
[7] S. Civiš, Y. Hosaki, E. Kagi, H. Izumuira, K. Yanagisawa, T. Šedivcová, and K. Kawaguchi, Publ. Astron. Soc. Jpn. **57,** 605 (2005).
[8] B. D. Rehfuss, D.-J. Liu, B. M. Dinelli, M.-F. Jagod, W. C. Ho, M. W. Crofton, and T. Oka, J. Chem. Phys. **89,** 129 (1988).
[9] P. Rosmus and H.-J. Werner, J. Chem. Phys. **80,** 5085 (1984).
[10] P. E. M. Siegbahn, J. Chem. Phys. **70,** 5391 (1980).
[11] H.-J. Werner and P. J. Knowles, J. Chem. Phys. **89,** 5803 (1988).
[12] P. J. Knowles and H.-J. Werner, Chem. Phys. Lett. **145,** 514 (1988).
[13] T. H. Dunning Jr, J. Chem. Phys. **90,** 1007 (1989).
[14] H.-J. Werner and P. J. Knowles, with contributions from R. D. Amos, A. Bernhardsson, A. Berning, P. Celani, D. L. Cooper, M. J. O. Deegan, A. J. Dobbyn, F. Eckert, C. Hampel, G. Hetzer, T. Korona, R. Lindh, A. W. Lloyd, S. J. McNicholas, F. R. Manby, W. Meyer, M. E. Mura, A. Nicklass, P. Palmieri, R. Pitzer, G. Rauhut, M. Schütz, H. Stoll, A. J. Stone, R. Tarroni, and T. Thorsteinsson, MOLPRO 2000.1, a package of *ab initio* programs, see http://www.molpro.net.
[15] F. Jenč, Int. Rev. Phys. Chem. **15,** 467 (1996).
[16] O. Bludský, M. Juřek, V. Špirko, B. A. Brandt, and F. Jenč, J. Molec. Spectrosc. **169,** 555 (1995).
[17] F. Jenč and J. Plíva, Collect. Czech. Chem. Commun. **28,** 1449 (1962).
[18] L. Ixaru, *Numerical Methods for Differential Equations and Applications* (Reidel, Dordrecht, 1984).
[19] G. Herzberg, *Molecular Spectra and Molcular Structure, I. Spectra of Diatomic Molecules* (Robert E. Krieger Publishing Company, Florida, 1989).
[20] P. Huber and G. Herzberg, *Constants of Diatomic Molecules* (Van Nostrand Reinhold, New York, 1979).
[21] R. D. Mead, J. Chem. Phys. **82,** 1723 (1985).
[22] P. L. Jones, J. Chem. Phys. **73,** 4419 (1980).
[23] G. Herzberg and A. Lagerqvist, Can. J. Phys. **46,** 2363 (1968).
[24] E. J. Bakker, L. B. F. M. Waters, H. J. G. L. M. Lamers, N. R. Trams, and F. L. A. VanderWolf, Astron. Astrophys. **310,** 893 (1996).
[25] R. Hirata and T. Horaguchi, Atomic spectral line list (1995).